Sister Rod Destructive Examinations (FY20)

Appendix B: Segmentation, Defueling, Metallographic Data and Total Cladding Hydrogen

Spent Fuel and Waste Disposition

Prepared for
US Department of Energy

Spent Fuel and Waste Science and Technology

Oak Ridge National Laboratory
Rose Montgomery, Robert N. Morris, Zachary Burns, Tyson Jordan, James T. Dixon, Stephanie M. Curlin, Jason Harp

November 30, 2020

M2SF-21OR010201032

ORNL/SPR-2020/1744

SUMMARY

This report documents work performed under the Spent Fuel and Waste Disposition's Spent Fuel and Waste Science and Technology program for the US Department of Energy (DOE) Office of Nuclear Energy (NE). This work was performed to fulfill Level 2 Milestone M2SF-21OR010201032, "ORNL High Burnup Confirmatory Demo Sibling Rod Testing Results," within work package SF-21OR01020103 and is an update to the work reported in M2SF-19ORO010201026 and M2SF-19OR010201028.

As a part of the DOE-NE High Burnup Spent Fuel Data Project, Oak Ridge National Laboratory (ORNL) is performing destructive examinations (DEs) of high burnup (HBU) (>45 GWd/MTU) spent nuclear fuel (SNF) rods from the North Anna Nuclear Power Station operated by Dominion Energy. The SNF rods, called *sister rods* or *sibling rods* are all HBU and include four different kinds of fuel rod cladding: standard Zircaloy-4 (Zirc-4), low-tin (LT) Zirc-4, ZIRLO®, and M5®. The DEs are being conducted to obtain a baseline of the HBU rod's condition before dry storage and are focused on understanding overall SNF rod strength and durability. Both composite fuel and defueled cladding will be tested to derive material properties. Although the data generated can be used for multiple purposes, one primary goal for obtaining the post-irradiation examination data and associated measured mechanical properties is to support SNF dry storage licensing and relicensing activities by (1) addressing identified knowledge gaps and (2) enhancing the technical basis for post-storage transportation, handling, and subsequent disposition of the SNF.

This report documents the status of the ORNL Phase 1 DE activities related to:

- Rough segmentation (RS)
- Defueling (DEF)
- DE.02 optical microscopy (MET)
- DE.03, cladding total hydrogen measurements

for seven Phase 1 sister rods and outlines the DE tasks performed and the data collected to date, as guided by the sister rod test plans.

Table SB-1 provides the status of the DE discussed in this appendix.

Table SB-1. DE status.

Planned DE		Status	ORNL lead	Comments
RS	Rough segmentation	Complete	Morris / Burns	All rough segmentation is complete for Phase 1 rods
DEF	Defueling	In progress	Montgomery	The majority of the defueling is complete. Additional defueling of DE.02 and DE.03 specimens as needed.
DE.02	Perform optical microscopy (MET)	In progress	Jordan (fueled); Dixon / Curlin (defueled)	Fueled and defueled specimens are being prepared for MET views. The Phase 1 priority 1 specimens were cut and specimen preparation/polishing is in progress. Cladding/pellet views and measurements are available for all Phase 1 rods. Specific features including waterside oxide thickness, remaining cladding wall thickness, pelletside oxide thickness, HBU rim, and cladding inner and outer diameter were measured. Where applicable, comparisons with nondestructive examinations were provided. Section views were inspected for hydride orientation and radial hydrides are visible in the heat-treated M5-clad specimen and the ZIRLO-clad heat-treated specimen. There is a high hydride density in the heat-treated Zirc-4 specimen. The few radial hydrides are short. The baseline ZIRLO-clad specimen includes short radial hydrides. The other baseline specimens did not have radial hydrides. An axial MET was created at a pellet-pellet gap. Axial and radial METs do not show a change in the hydride precipitation density through the gap. A section of the cladding will be analyzed for total hydrogen content to determine whether the total cladding hydrogen content varies between the pelleted region and the pellet-pellet gap. Other rod elevations are slated for MET views and the work will continue.
DE.03	Cladding total hydrogen measurements	Equipment verification and calibration	Harp	Specimens were defueled and the equipment was set up. Out of cell verification testing of the oxygen nitrogen hydrogen analyzer is underway and cladding measurements are expected to follow in early FY21.

ACKNOWLEDGMENTS

Many thanks to our US Department of Energy Office of Nuclear Energy sponsor, Ned Larson, along with the Spent Fuel and Waste Science and Technology (SFWST) storage and transportation program leadership for their continued support. The sister rod project would not be possible without the vision and support of the Electric Power Research Institute, Westinghouse, Framatome, and Dominion Energy.

This work would not be possible without the support and expertise provided by the leadership and staff members of the Oak Ridge National Laboratory's (ORNL's) Irradiated Fuel Examination Laboratory (IFEL). Special thanks go to John Hinds and Brian Woody, the 3525 operators, Tracy Binger, and Mark Walls for their assistance with the defueling, cleaning, and irradiated material handling. Rick Henry has the unenviable task of tracking the bits and pieces of sister rods and their moves around the hot cell and to other facilities, and we very much appreciate his patience and continued support.

Special thanks go to Tyler Smith for his work developing a defueling column for the sister rod fuel material. We appreciate his continuing support, and the ongoing efforts from Lindsey Aloisi to defuel the many small specimens required for total cladding hydrogen and metallographic studies. We also appreciate Tracy Binger's efforts measuring and tracking the defueled cladding radiation levels in support of releasing the specimens to ORNL's Low Activation Materials Development and Analysis (LAMDA) lab. Our appreciation and thanks are extended to Josh Schmidlin, Thomas Muth, and the LAMDA lab staff for their continuing support on the sister rod metallography. For his wise advice and support deploying new equipment and processes at IFEL, we appreciate Jim Miller.

This page is intentionally left blank.

CONTENTS

This page is intentionally left blank.

LIST OF FIGURES

LIST OF TABLES

This page is intentionally left blank.

REVISION HISTORY

Date	Changes
3/29/2019	Initial release
9/27/2019	Revised to include additional data and incorporate comments from the previously released report.
10/30/2020	Initial release of this appendix.
11/30/2020	The document numbering was revised to reflect its M2 status and the date was changed.

This page is intentionally left blank.

ACRONYMS

CIRFT	Cyclic Integral Reversible Fatigue Tester
DE	destructive examination
DOE	US Department of Energy
EPRI	Electric Power Research Institute
FHT	full-length fuel rod heat treatment
FY	fiscal year
GTRF	grid-to-rod fretting
HBU	high burnup
ID	inner diameter
IFEL	Irradiated Fuels Examination Laboratory
LT	low tin
LVDT	linear variable differential transducer
MET	metallography
NE	Office of Nuclear Energy
NDE	nondestructive examination
OD	outer diameter
ONH	oxygen nitrogen hydrogen
ORNL	Oak Ridge National Laboratory
PWR	pressurized water reactor
RPC	Research Project Cask
RS	rough segmentation
SNF	spent nuclear fuel

This page is intentionally left blank

B-1. ROUGH SEGMENTATION (RS)

Seven Phase 1 rods [B-1,B-2,B-3] were segmented:

- 30AD05 (M5 clad)
- 30AE14 (M5 clad, heat-treated)
- 3D8E14 (ZIRLO clad)
- 3F9N05 (ZIRLO clad, heat-treated)
- F35P17 (Zirc-4 clad, heat-treated)
- 3A1F05 (LT Zirc-4 clad)
- 6U3K09 (ZIRLO clad)

A detailed cutting plan was developed [B-3], with test specimens allocated for the destructive examinations (DE) as guided by the test plans [B-2,B-3] and the results of the nondestructive examination (NDE) [B-4]. Each segment was marked to indicate the upper elevation and placed into a labeled storage capsule as it was cut. The capsules are not backfilled with inert gas because these Phase 1 rod segments are expected to be used in testing within a few years. The rough segments are further subdivided as needed for the slated DE.

This page is intentionally left blank.

B-2. DEFUELING (DEF)

Many segments will be defueled in the process of specimen preparation for DE. For example, all DE.03 specimens must be defueled before testing. DE.10 includes fueled and defueled specimens. In some cases, the removed fuel is the target of the test (e.g., DE.01 includes burnup measurements). The defueling processes vary depending on the follow-on tests to be performed. This section briefly describes defueling activities.

B-2.1 Defueling Cladding Segments for Argonne National Laboratory Shipment

Twelve rod cladding segments were selected from the Phase 1 sister rods for ring compression testing as listed in Table B-1. The segments were defueled by boiling them individually in an acid bath, and each piece of defueled cladding was weighed and packaged individually in aluminum containers. The dose rate was measured at contact and at 1 ft. The dose rates represent the hottest spots on the container. The exterior surfaces of the aluminum containers were decontaminated before they were loaded into the shipping container. The dose rate of a decontaminated empty aluminum container is expected to be <20mR/hr. Figure B-1 shows the cladding segments in their aluminum containers awaiting shipment to Argonne National Laboratory and a dose rate measurement being taken on one sample in its aluminum container using a Ludlum 9-4 ion chamber.

To determine the isotopic inventory of any pellet materials that might still be adhered to the interior wall of the cladding following this defueling process, one 18 mm rod segment was defueled using the same process, and then the resulting defueled cladding segment was dissolved and analyzed. The results of the analysis, tabulated in Table B-2, were used to determine the residual pellet material isotopic content of each cladding segment based on the segment's weight.

Shipment of the segments was completed in April 2019.

Table B-1. Defueled cladding specimens for shipment to Argonne National Laboratory

Sister rod and elevation of segment	Aluminum canister weight (g)	Canister + clad weight (g)	Clad weight (g)	Gamma dose on contact (mR/h)	Gamma dose @ 30cm (mR/h)
30AD05-2429-2519-DE.10	10.18	19.20	9.02	1,800	70
30AD05-3259-3349-DE.10	9.97	19.04	9.07	1,800	70
30AE14-2694-2784-DE.10	10.19	19.55	9.36	2,300	100
30AE14-3309-3399-DE.10	10.39	19.76	9.37	1,800	70
3A1F05-2555-2645-DE.10	10.22	19.74	9.52	1,200	50
3A1F05-3015-3105-DE.10	10.41	19.79	9.38	1,000	40
3D8E14-2213-2303-DE.10	10.17	19.68	9.51	1,400	60
3D8E14-2565-2655-DE.10	10.16	19.74	9.58	1,400	60
3F9N05-2572-2662-DE.10	10.22	19.78	9.56	1,400	70
3F9N05-3241-3331-DE.10	10.02	19.60	9.58	1,200	50
F35P17-2555-2645-DE.10	10.16	19.42	9.26	1,200	40
F35P17-3069-3159-DE.10	10.14	19.91	9.77	1,000	40

Table B-2. Residual pellet materials after defueling on an activity per gram of cladding basis

Isotope	Ci/g	Isotope	Ci/g	Isotope	Ci/g
Co-60	7.20E-06	Np-237	2.14E-10	Pu-242	4.81E-09
Zr-95	4.15E-06	U-234	3.70E-10	Am-241	2.85E-06
Ru-106	2.08E-05	U-235	3.87E-12	Am-242m	2.44E-08
Sb-125	1.27E-05	U-236	1.07E-10	Am-243	6.47E-08
Cs-134	1.58E-04	U-238	7.19E-11	Cm-244	1.04E-05
Cs-137	1.27E-03	Pu-238	3.53E-06	Cm-245	2.41E-09
Ce-144	4.15E-06	Pu-239	3.75E-07	Cm-246	9.61E-10
Eu-154	5.53E-05	Pu-240	5.33E-07	Beta *	3.708E-03
Eu-155	1.94E-05	Pu-241	0.000147		

* "Beta" is the remaining beta activity after subtracting known beta emitters and G-Alpha results from liquid scintillation result. It is assumed to represent Sr-90/Y-90.

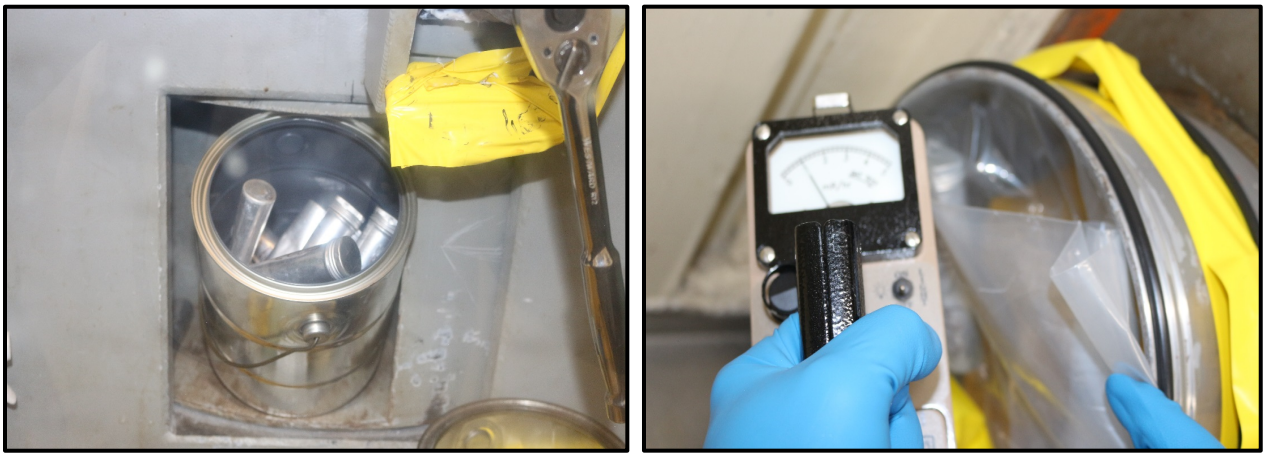

Figure B-1. Defueled cladding segments in aluminum containers awaiting shipment to ANL (left) and contact dose rate measurement on a single container (right).

B-2.2 Defueling Cladding Segments to Prepare Total Cladding Hydrogen and Metallographic Specimens

To prepare specimens for total cladding hydrogen measurements (DE.03), the fuel is removed from the cladding. Also, it is desired to produce some cladding-only metallographic (DE.02) specimens. To remove the fuel from the cladding for these examinations, a dissolution column was constructed and installed in the IFEL hot cell in March 2019. The column, shown in Figure B-2, incorporates a recirculating acid loop to reduce the volume of waste generated and reduce acid vapor released to the hot cell atmosphere. The design also includes a Soxhlet extractor that periodically flushes the dissolution acid bath from the chamber in which the cladding is held. This provides a supply of clean acid to remove as much fuel as possible. Figure B-2(a) shows a defueled specimen planned for metallographic imaging, and Figure B-2(b) shows the dissolution column in the ORNL hot cell. To date, 13 specimens were defueled using the dissolution column.

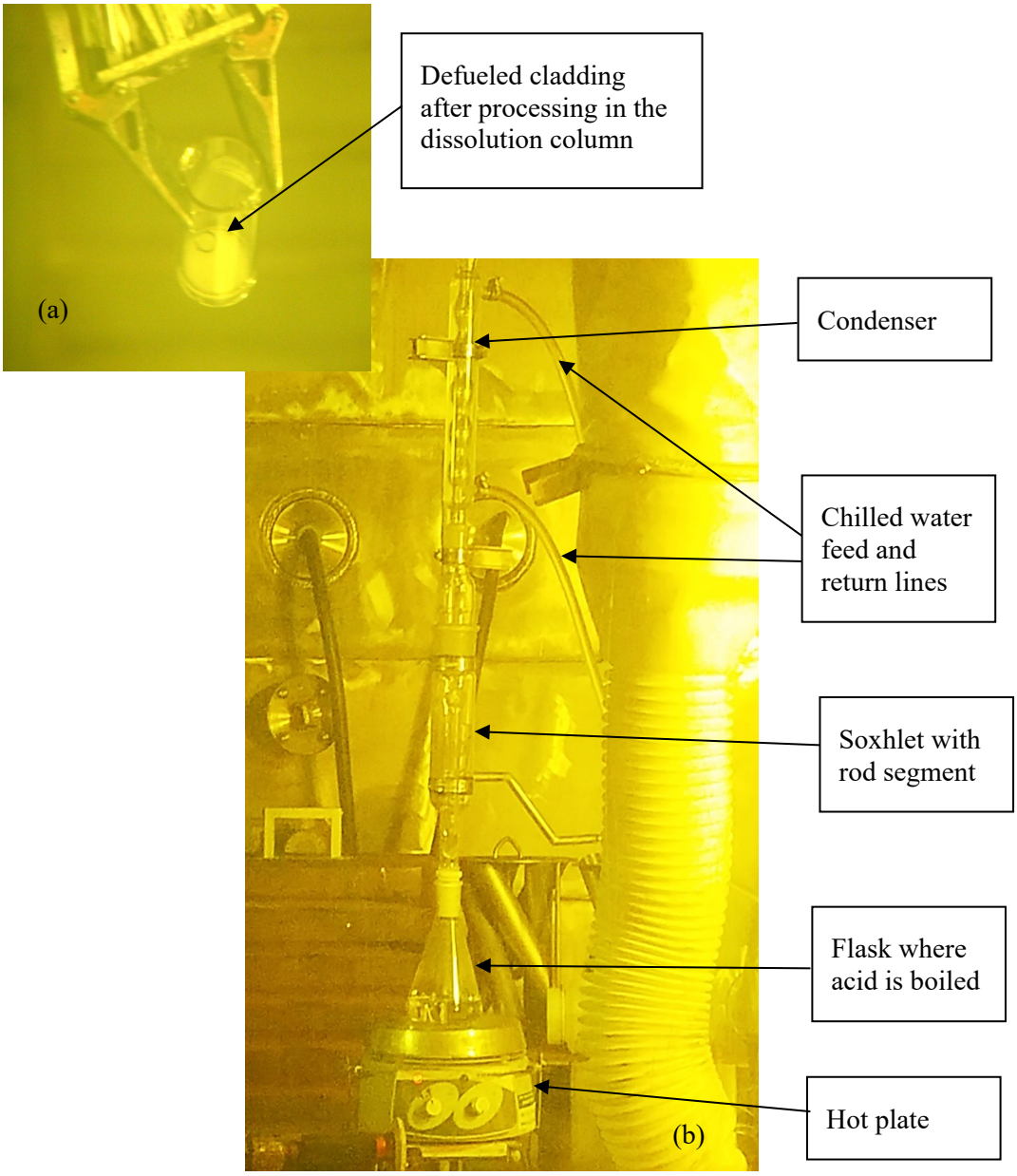

Figure B-2. (a) A Defueled Specimen Ready for DE.02 or DE.03 after Several Passes in (b) the Dissolution Column Installed in the ORNL IFEL Hot Cell.

This page is intentionally left blank.

B-3. METALLOGRAPHY (DE.02)

The rough-cut DE.02 segments provide source material for several exams, including metallographic mounts (METs), total cladding hydrogen analysis, microhardness, scanning electron microscope (SEM), and transmission electron microscope (TEM) imaging. The first step in the DE.02 process is to cut appropriate specimens from the segments for each exam. Approximately ⅓ of the Phase 1 DE-02 segments were sub-sectioned.

For METs, defueled and fueled views were prepared. The fueled views allow pellet features such as cracks and the HBU rim to be inspected, while the defueled views typically provide much cleaner and clearer views of the cladding with its hydrides and oxide layers. Figure B-3 provides examples of the typical features discussed within the METs. Not all features are visible in all views. For example, pellet cracks are only visible in fueled full-section METs, as shown in the upper right of Figure B-3. If a feature in the image is straight, then it is likely a polishing artifact or scratch. The waterside and pelletside can usually be identified by the curvature of the cladding when the pellet is not present. The waterside oxide usually appears flat in cross-sectional METs and the pelletside oxide appears wavy where the oxide has grown into the pellet. Cladding hydride precipitates are either dark lines (when defueled and etched) or white lines (in the fueled METs) either follow the curvature of the cladding or are perpendicular to it. In fueled MET views, pellet porosity is visible as dark spots in the pellet region. For clarity, these typical features are not labeled in every MET and only atypical features are labeled where necessary.

Table B-3 summarizes the Phase 1 DE.02 segments and selected metallographic views, selected specimens for total cladding hydrogen measurements, and the current status of the exams.

METs are available for all 7 of the Phase 1 Sister Rods but not all planned elevation views are available. The available views are organized by cladding type in Sections B-3.1 through B-3.4. A summary of cladding thickness, waterside oxide thickness, pellet-side oxide thickness, and HBU rim measurements taken using the MET views are provided in Table B-4 by rod and elevation where available. The minimum remaining wall thickness was measured as 495 μm for 3A1F05, and the thickest waterside oxide thickness was 128 μm for the same rod, which also had extensive oxide spalling.

The NDE provided rod outer diameter (OD) measurements using linear variable differential transducers (LVDTs) and waterside oxide thickness and minimum remaining cladding wall thickness measurements using eddy current methods [B-4]. The LVDT-reported OD seems to be biased on the high side by ~2%. Likewise, the eddy current measurements of remaining wall thickness seem to be biased ~4% on the high side, except for the Zirc-4 and LT-Zirc 4-clad rods. For those cladding alloys, eddy current measured wall thickness was lower than that measured using the METs. The eddy current estimated remaining wall thickness for 3A1F05-2735-2754 is ~10% lower than that measured using the METs. As discussed in the NDE report [B-4], the waterside oxide thickness varies around the circumference of the cladding. Generally, the maximum recorded MET measurements are comparable with the local average eddy current oxide thickness measurements, except for the M5-clad rods. The M5-clad rods had very low oxide thickness in the lower ranges of detectability for the eddy current system used.

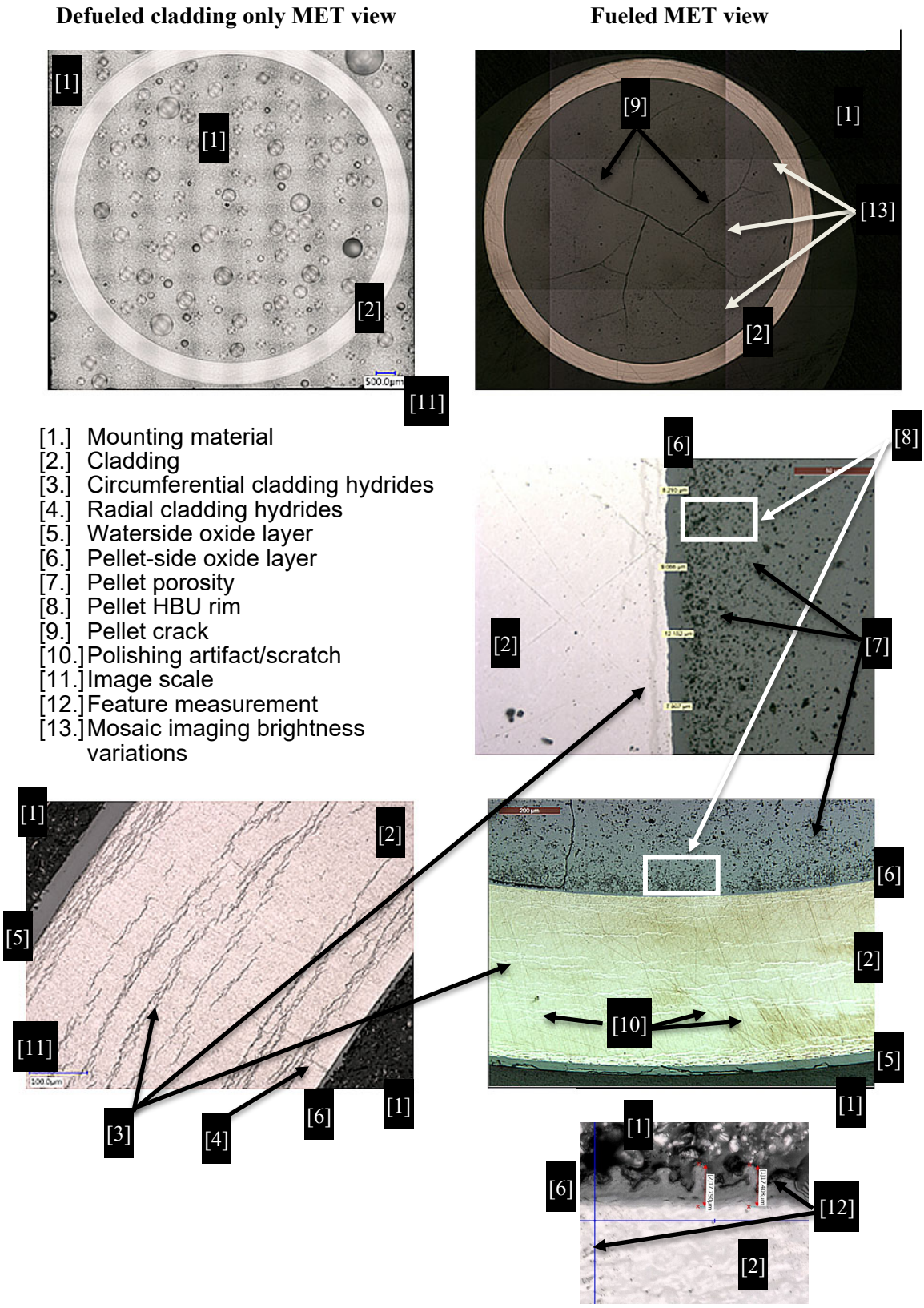

Figure B-3. Example of typical MET views and section features.

Table B-3. Phase 1 DE.02 parent segments with metallographic and total cladding hydrogen specimen selections and status.

Rod and originating segment elevation range (mm)			Fueled or defueled MET	Selection criteria	MET	Total cladding H_2
30AD05	678	697	TBD	Oxide thickness	✓	
30AD05	1,280	1,299	Fueled	Oxide thickness	Mounted	✓
30AD05	2,410	2,429	Defueled	HBU region with higher oxide	Specimen cut	✓
30AD05	2,783	2,802	Fueled	HBU region	Mounted	✓
30AD05	3,240	3,259	Both	Highest oxide	Complete	✓
30AE14	653	672	TBD	Oxide thickness	✓	
30AE14	1,677	1,696	Defueled	Oxide thickness	Specimen cut	✓
30AE14	2,203	2,222	Defueled	HBU at oxide peak	Specimen cut	
30AE14	2,675	2,694	Both	HBU at oxide peak	Fueled complete, defueled specimen cut	✓
30AE14	3,399	3,418	Both	Highest oxide thickness	Complete	✓
3A1F05	1,260	1,279	Fueled	Oxide thickness	Complete	
3A1F05	1,585	1,604	Fueled	Oxide thickness	Complete	
3A1F05	2,006	2,025	Defueled	Oxide thickness	Specimen cut	✓
3A1F05	2,383	2,402	Defueled	HBU with higher oxide thickness, spalling oxide, pellet banding	Specimen cut	✓
3A1F05	2,735	2,754	Both	High oxide thickness at HBU	Complete	✓
3A1F05	3,105	3,124	Defueled	Peak oxide thickness	Defueled but unable to complete due to unexpected high dose rates	✓
3D8E14	700	719	Fueled	Oxide thickness	Mounted	
3D8E14	1,178	1,331	Fueled	Fretting mark depth (post fatigue test)	Mounted	
3D8E14	1,375	1,450	Fueled	Pellet-pellet gap and oxide thickness	Complete	✓
3D8E14	2,303	2,322	Defueled	Oxide thickness	Specimen cut	
3D8E14	2,655	2,674	Defueled	HBU with oxide spike	Complete	✓
3D8E14	3,206	3,225	Both	Highest oxide thickness	Fueled mounted/ defueled complete	✓
3F9N05	700	719	Defueled	Oxide thickness	✓	
3F9N05	1,425	1,444	Defueled	Oxide thickness	Specimen cut	✓
3F9N05	2,300	2,329	Defueled	Oxide thickness	Mounted	
3F9N05	2,863	2,882	Defueled	HBU with higher oxide	Complete	✓
3F9N05	3,331	3,350	Both	Peak oxide thickness and spalling oxide	Complete	✓
6U3K09	2,616	2,635	Fueled	CIRFT correlating data	Complete	
6U3K09	3,506	3,525	Fueled	CIRFT correlating data	✓	
F35P17	911	930	TBD	Oxide thickness	✓	
F35P17	1,300	1,319	Defueled	Oxide thickness	Specimen cut	✓
F35P17	2,008	2,027	TBD	HBU with higher oxide thickness	✓	
F35P17	2,383	2,402	Defueled	Oxide thickness, spalling oxide	Specimen cut	
F35P17	2,735	2,754	Both	Oxide thickness and spalling oxide	Complete	✓
F35P17	3,050	3,069	Both	Peak oxide thickness and spalling oxide	✓	✓

✓ Planned but not yet started.

Table B-4. Summary of metallographic section measurements obtained to date.

Shaded cells indicate measurement is unavailable.

Some METs were imaged but not measured and they are not included in this table.

Rod ID and original section elevations (mm)			Cladding type	Heat-treated rod?	Estimated local burnup (GWd/MTU)	Average measured cladding thickness (µm)	Maximum measured (µm)	Minimum measured (µm)	Measured waterside oxide thickness (µm)	Maximum measured (µm)	Minimum measured (µm)	Measured Pellet side oxide thickness (µm)	Maximum measured (µm)	Minimum measured (µm)	Measured HBU rim thickness (µm)	Maximum measured (µm)	Minimum measured (µm)	Average measured Rod Outer diameter (mm)	Maximum measured (mm)	Minimum measured (mm)	Measured Cladding Inner diameter (mm)	Maximum measured (mm)	Minimum measured (mm)
30AD05	3240	3259	M5	no	55	541	546	535	12	13	11	11	14	7	57	70	43	9.389	9.416	9.374	8.279	8.288	8.273
30AE14	2675	2694	M5	yes	61	560	575	541	9	10	8	13	18	10				9.389	9.416	9.374	8.279	8.288	8.273
30AE14	3399	3418	M5	yes	50	562	585	545	12	15	10	10	16	8	61	82	42	9.419	9.449	9.398	8.310	8.338	8.283
3D8E14	2655	2674	ZIRLO	no	64	549	564	531	34	41	31	15	18	12	70	108	52	9.466	9.495	9.424	8.330	8.344	8.306
6U3K09	2616	2635	ZIRLO	no	58	560	571	549	21	22	19	9	12	6	59	107	36	9.440	9.455	9.425	8.276	8.302	8.249
3F9N05	2863	2882	ZIRLO	yes	58	554	563	547	30	38	24	12	16	8				9.450	9.450	9.449	8.277	8.277	8.275
3F9N05	3331	3350	ZIRLO	yes	51	554	559	544	39	60	27	9	12	6	35	51	27	9.480	9.496	9.464	8.271	8.271	8.270
3A1F05	1260	1279	LT Zirc-4	no	56	560	565	555	15	18	14	10	12	7	54	74	43	9.436	9.436	9.436	8.299	8.299	8.299
3A1F05	2735	2754	LT Zirc-4	no	54	546	630	495	90	128	43	12	16	9	72	90	62	9.485	9.548	9.421	8.290	8.300	8.280
F35P17	2735	2754	Zirc-4	yes	66	524	591	510	81	86	73	15	27	10	101	115	94	9.438	9.517	9.385	8.319	8.366	8.274

Table B-5. Comparison of Metallographic Section Measurements with Nondestructive Measurements

Rod ID and original section elevations (mm)			NDE measured local OD using LVDT (mm)	MET measured average OD (mm)	Differential OD (LVDT – MET) (mm)	NDE Measured Local waterside oxide thickness (µm)	MET maximum measured oxide thickness (µm)	Differential waterside oxide thickness (NDE – MET) (µm)	NDE measured wall thickness (µm)	MET measured wall thickness (µm)	Differential Wall thickness (NDE-MET) (µm)
30AD05	3,240	3,259	9.420	9.389	0.031	20	13	7	572	541	31
30AE14	2,675	2,694	9.459	9.389	0.070	16	10	6	576	560	16
30AE14	3,399	3,418	9.440	9.419	0.021	23	15	9	574	562	12
3D8E14	2,655	2,674	9.517	9.466	0.051	42	41	1	570	549	21
6U3K09	2,616	2,635	9.474	9.440	0.034	22	22	0	566	560	6
3F9N05	2,863	2,882	9.482	9.450	0.032	45	38	7	564	554	9
3F9N05	3,331	3,350	9.478	9.480	-0.002	60	60	0	560	554	6
3A1F05	1,260	1,279	9.475	9.436	0.039	21	18	3	541	560	-19
3A1F05	2,735	2,754	9.564	9.485	0.080	137	128	9	490	546	-56
F35P17	2,735	2,754	9.549	9.438	0.111	88	86	2	503	524	-21

B-3.1 M5-Clad Sister Rods

Five MET views from three elevations are currently available for the two Phase 1 M5-clad sister rods, 30AD05 (as received baseline condition) and 30AE14 (full-length rod heat treatment (FHT) applied), as shown in Figures B-4 through B-9. 30AD05 and 30AE14 provide a good comparison, since they were from the same fuel assembly, were manufactured at the same time by the same fuel vendor, had the same irradiation history and are only 5 GWd/MTU different in average burnup at the elevations examined.

The precipitated hydrides in the baseline M5-clad rod (30AD05) are homogeneously distributed through the thickness of the cladding and are oriented circumferentially. The pellet is cracked radially (as expected) with no missing pellet surface. The depth of the pellet HBU rim is 57 μm on average for the baseline rod (3,240 – 3,259 mm in elevation).

For the heat-treated M5-clad rod, many radial hydrides are visible, particularly at the inner diameter (ID) of the cladding. They appear to have preferentially precipitated at locations where a pellet crack exists at the cladding ID, as illustrated in Figure B-7's colorized view. The cladding is not supported by the pellet at the pellet crack and this results in a higher local stress concentration. The higher stress field provides a preferential location for hydride precipitation. The pellet cracks are as expected with no missing pellet surface. The HBU rim is 61 μm on average.

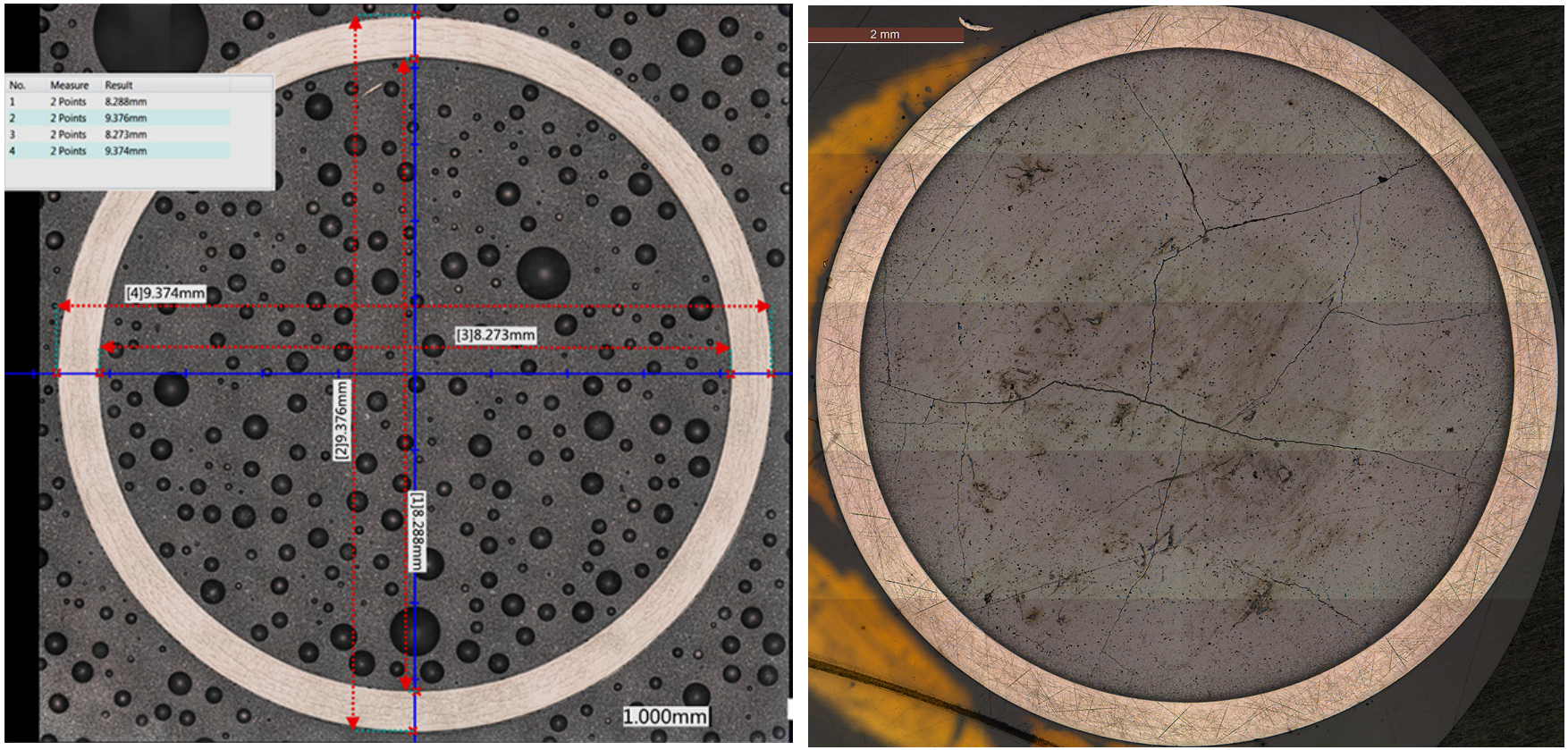

Figure B-4. Fueled (right) and defueled (left) overall section views, 30AD05-3240-3259 (baseline rod)

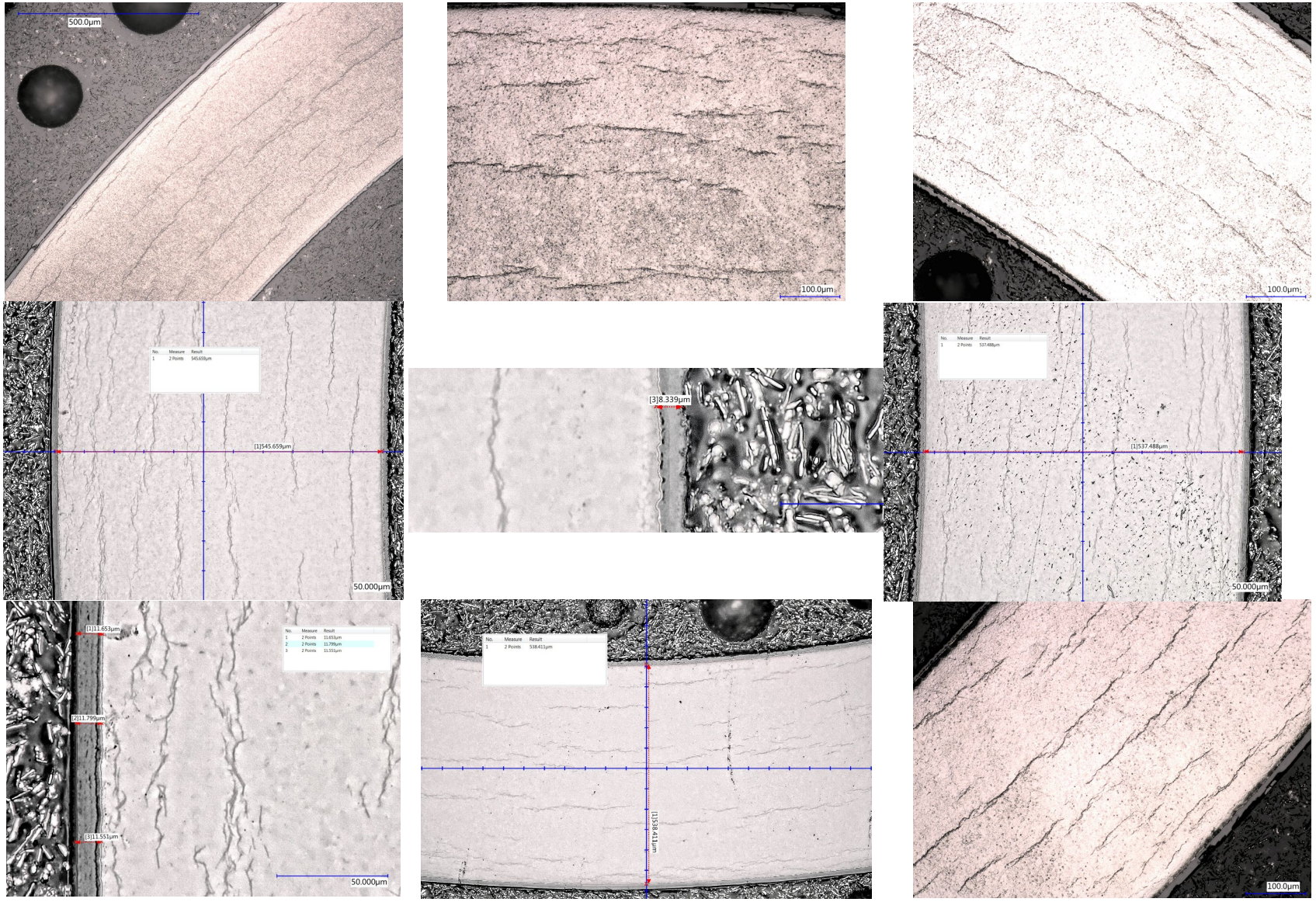

Figure B-5. Magnified areas of the cladding, 30AD05-3240-3259 (baseline rod).

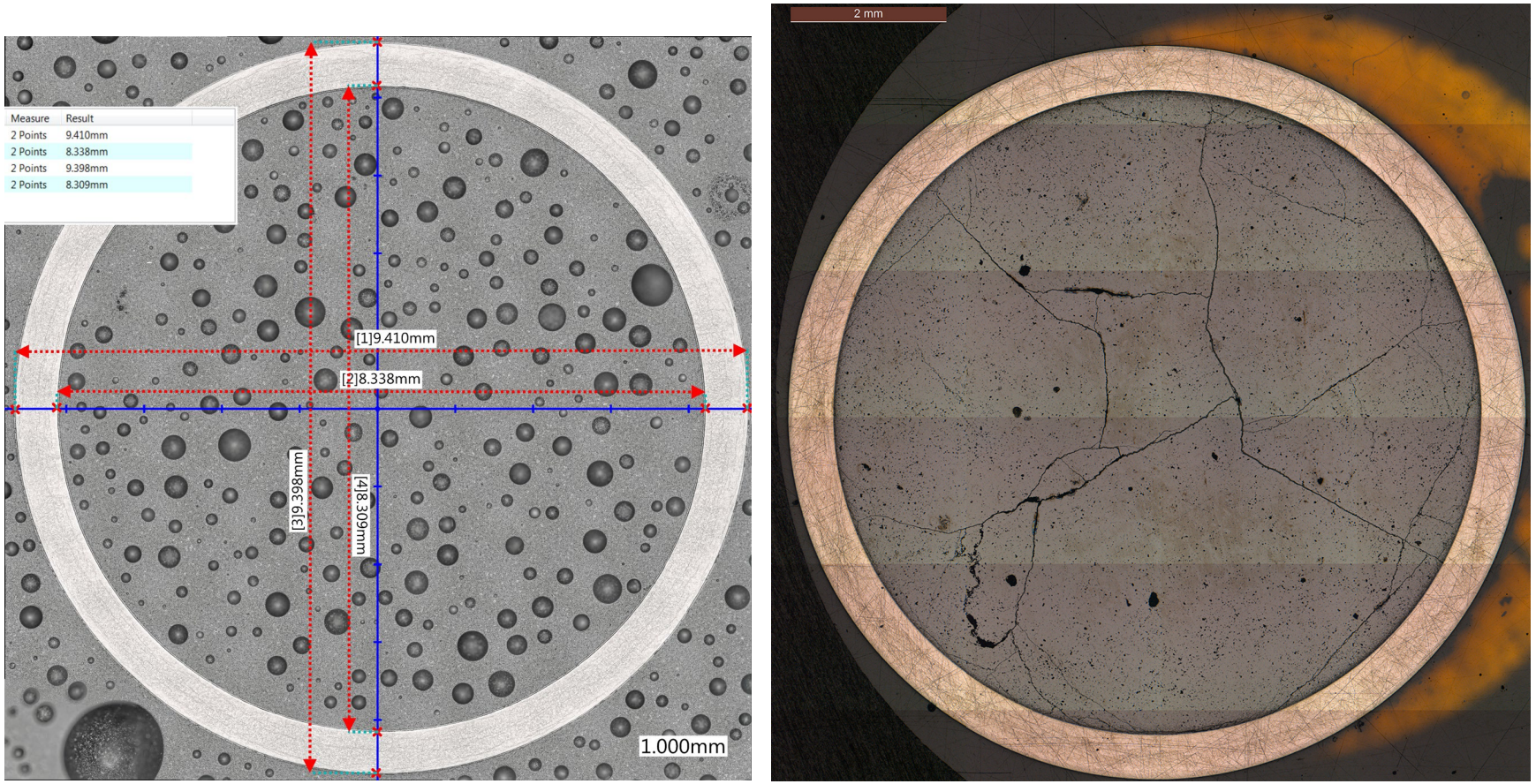

Figure B-6. Fueled (right) and defueled (left) overall section views, 30AE14-3399-3418 (heat treated rod).

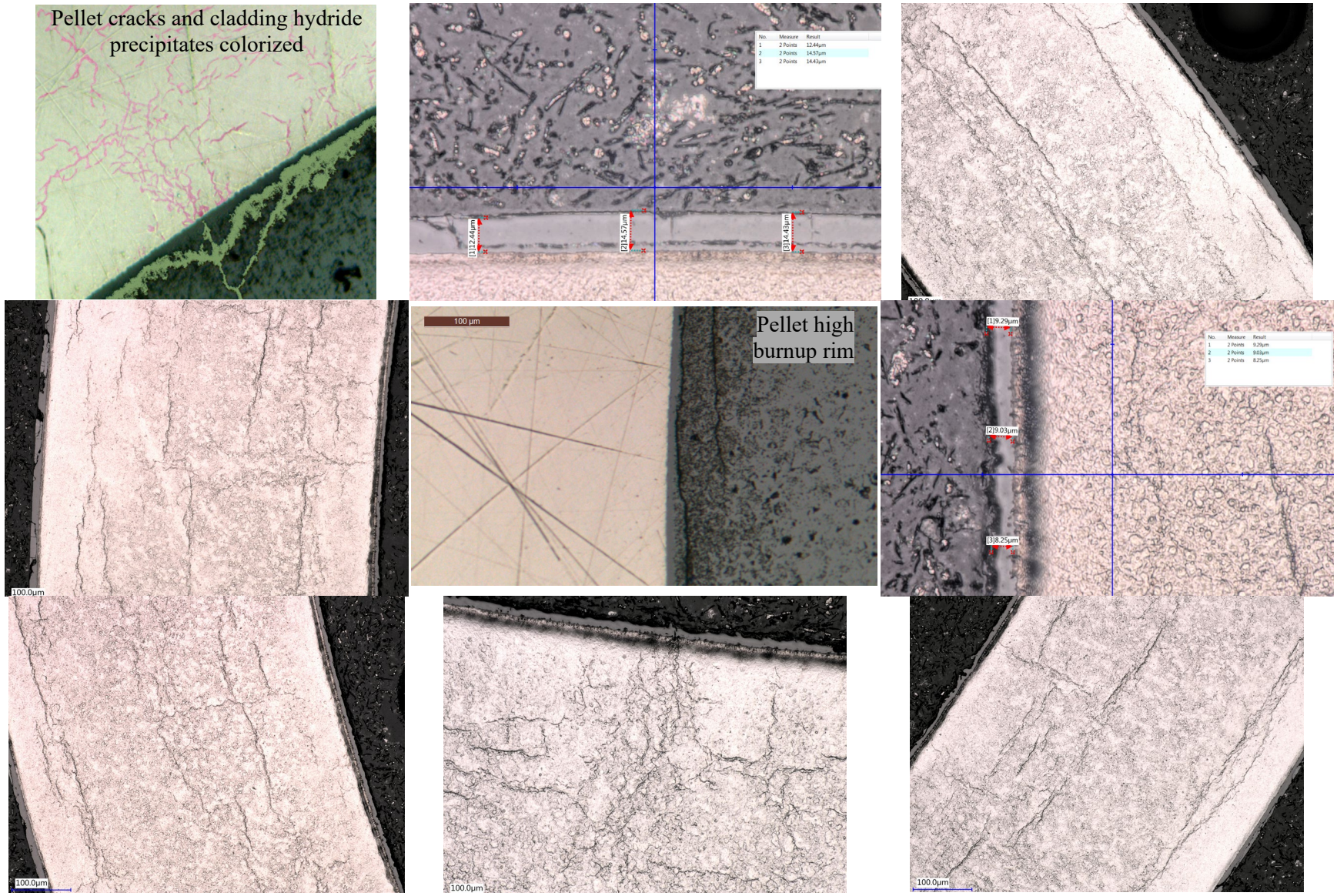

Figure B-7. Magnified views, 30AE14-3399-3418 (heat treated rod).

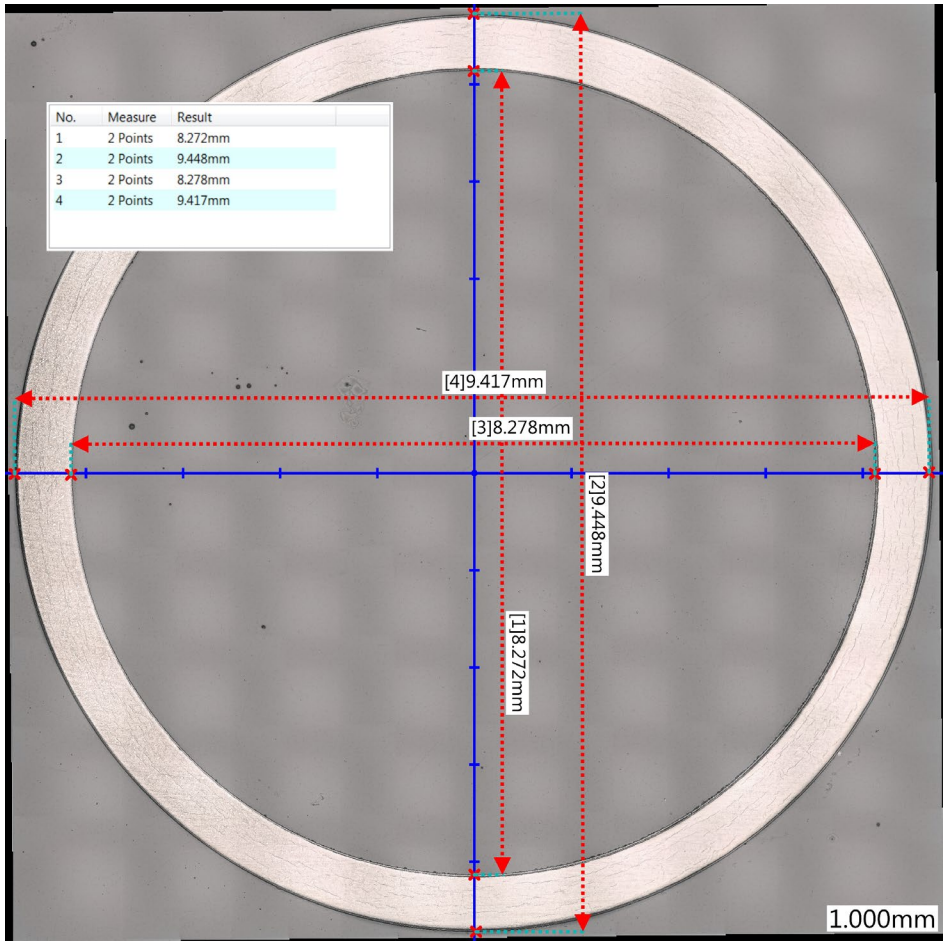

Figure B-8. Defueled overall view, 30AE14-2675-2694 (heat-treated).

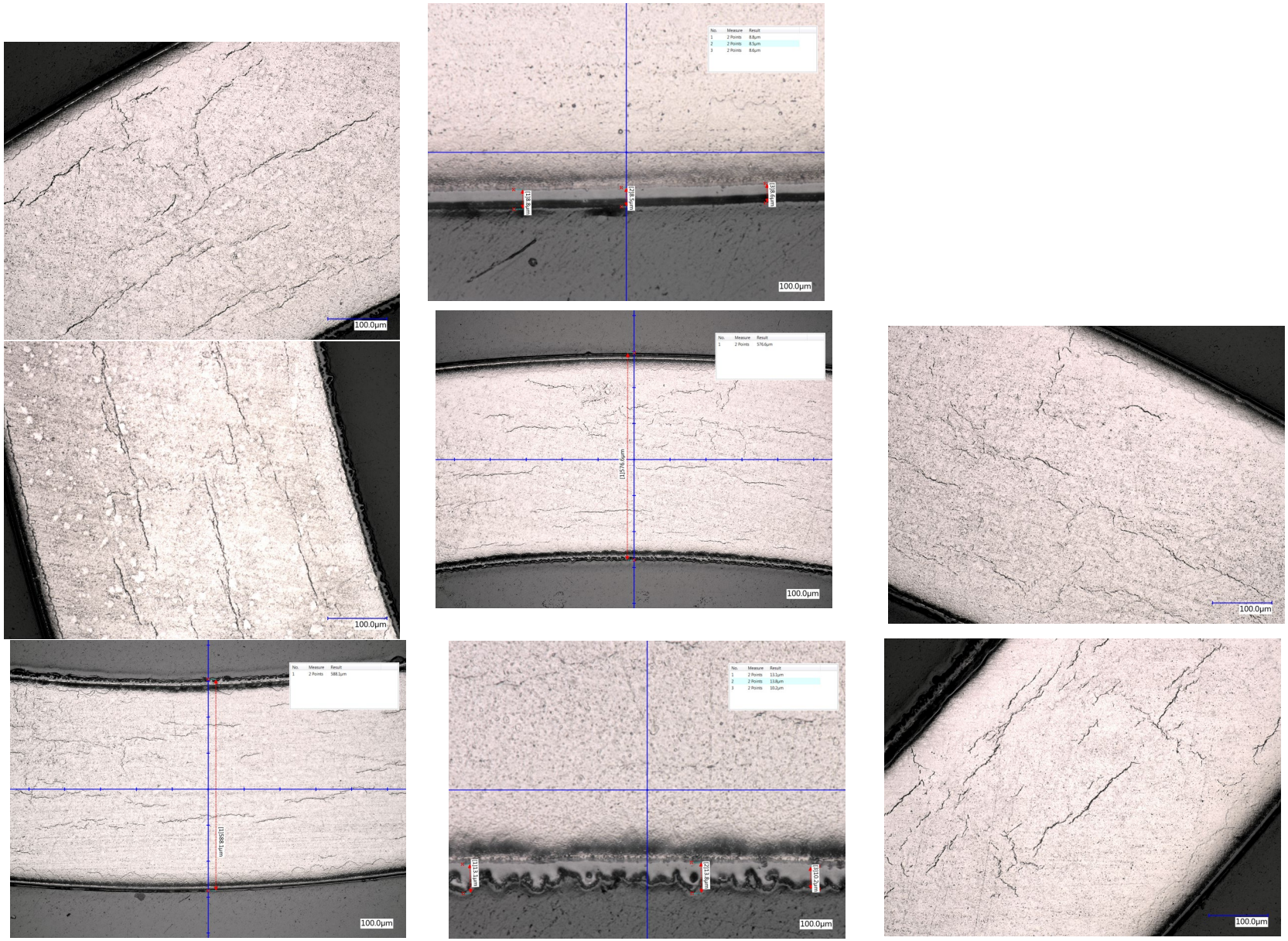

Figure B-9. Magnified areas of the cladding, 30AE14-2675-2694 (heat-treated).

B-3.2 ZIRLO-Clad Sister Rods

Eight MET mounts are available for the three Phase 1 ZIRLO-clad sister rods: 3D8E14 and 6U3K09 (as received baseline rods) and 3F9N05 (FHT applied). Figures B-10 through B-14 provide views of the baseline rods and Figures B-15 through B-19 provide views of the heat-treated rod. The three rods examined were from the same fuel vendor but were manufactured at different times and operated in different reactor cycles. At the elevations examined, the difference in estimated burnup ranges from 0 to 13 GWd/MTU (see Table B-4).

The precipitated hydrides in the baseline ZIRLO-clad rods (3D8E14 and 6U3K09) are primarily located at the OD and ID of the cladding and are oriented circumferentially. For 3D8E14, there are many short hydrides in the central region of the wall that form a cross pattern and there are several relatively long radial hydrides located at the cladding ID, as shown in Figures B-11 and B-12. 6U3K09 was not polished well enough to fully visualize the cladding hydrides, although there is a deeper OD field of circumferential hydrides (Figure B-14). The 6U3K09 pellet is cracked in the expected pattern with no missing pellet surface visible. The depth of the pellet HBU rim is 59 μm on average for the baseline rod (2,616 – 2,635 mm in elevation).

For the heat-treated ZIRLO-clad rod, the circumferential hydrides are more regularly distributed through the wall section, as shown in Figures B-16 and B-19, perhaps indicating hydrogen migration during the heat treatment. Several radial hydrides are visible at the ID and near the OD of the cladding. Because the polish on the fueled MET is not fine enough to fully visualize all of the hydrides, it is difficult to assess the preference for hydride precipitation at pellet crack locations. However, an inspection of magnified areas of the fueled MET (provided in Figure B-17) seems to indicate radial hydrides at pellet crack locations. This MET will be further processed and etched to better highlight the hydrides. The pellet cracks are as expected with no messing pellet surface. The HBU rim is 35 μm on average.

A pellet-pellet gap of 3 mm was identified at 1,403mm in elevation during the NDE [B-4]. The rod was sectioned axially at that elevation to reveal the pellet-pellet interfaces and the gap and to allow for additional examination of the pellet and cladding condition as related to the gap. An axial slice of the rod (approximately one third of the rod OD) was removed to reveal the pellets and was reserved for cladding hydrogen measurements. The resulting segment was then mounted and polished and the gap measured optically, as shown in Figure B-20. The gap is actually less than 1 mm as shown in Figure B-20(a) and was overestimated by the gamma scan likely due to the chamfers and dishes in the pellets. The axial specimen is slightly tilted its mount, giving the appearance of a taper as shown in Figure B-20(b). Because of the tilt and the off-center cut location the diameter measurements are not accurate. Axial measurements are less affected but still inaccurate. The axial view allows both axial and radial pellet cracks that occurred during reactor operation to be inspected. The pellet HBU rim is easily discernable and is enhanced at the pellet chamfer locations. The lower pellet has a small chip that relocated within the dish region as shown at the left end of Figure B-20(b). At least one chamfer has loose chips as shown at the right end of Figure B-20(b). Figure B-21 provides closer views of these details and provides a view of the hydride distribution just inside the cladding ID. The ID cladding oxide layer is discontinuous at the pellet-pellet gaps, and although some pellet material appears to be well bonded with the cladding ID oxide, there is a continuous crack in the pellet that keeps the pellet and cladding from fully functioning as a solid mechanical section. Following axial imaging, the specimen was cross sectioned to allow views in the gap (Figure B-20[d]) and above (Figure B-20[e]) and below it (Figure B-20[c]). The OD, ID, oxide layers, cladding wall thickness, and pellet HBU rim were measured on the cross-sectional METs and are provided in Table B-6. For comparison, the intact rod OD measured during NDE using LVDTs is also listed in Table B-6. The pre-cut OD matches within 4 μm in the pellet elevations, but after cutting the MET-measured OD in the gap region is 8.8 μm larger. It isn't clear whether some residual strain was released in the gap after cutting or whether this is measurement uncertainty. Figure B-21 provides examples of the hydride distribution in the cladding (a) above the gap in the pellet body, (b) in the gap, and (c) below the gap in the pellet body. Although the

section above the gap was not fully polished and the central portion of the wall is thus not useful for comparison, there is not a visual difference in the hydride distribution in the gap as compared with the cladding in the pellet body region. Total cladding hydrogen measurements will be performed to better quantify any additional hydrogen (in solution or precipitated) in the pellet-pellet gap region.

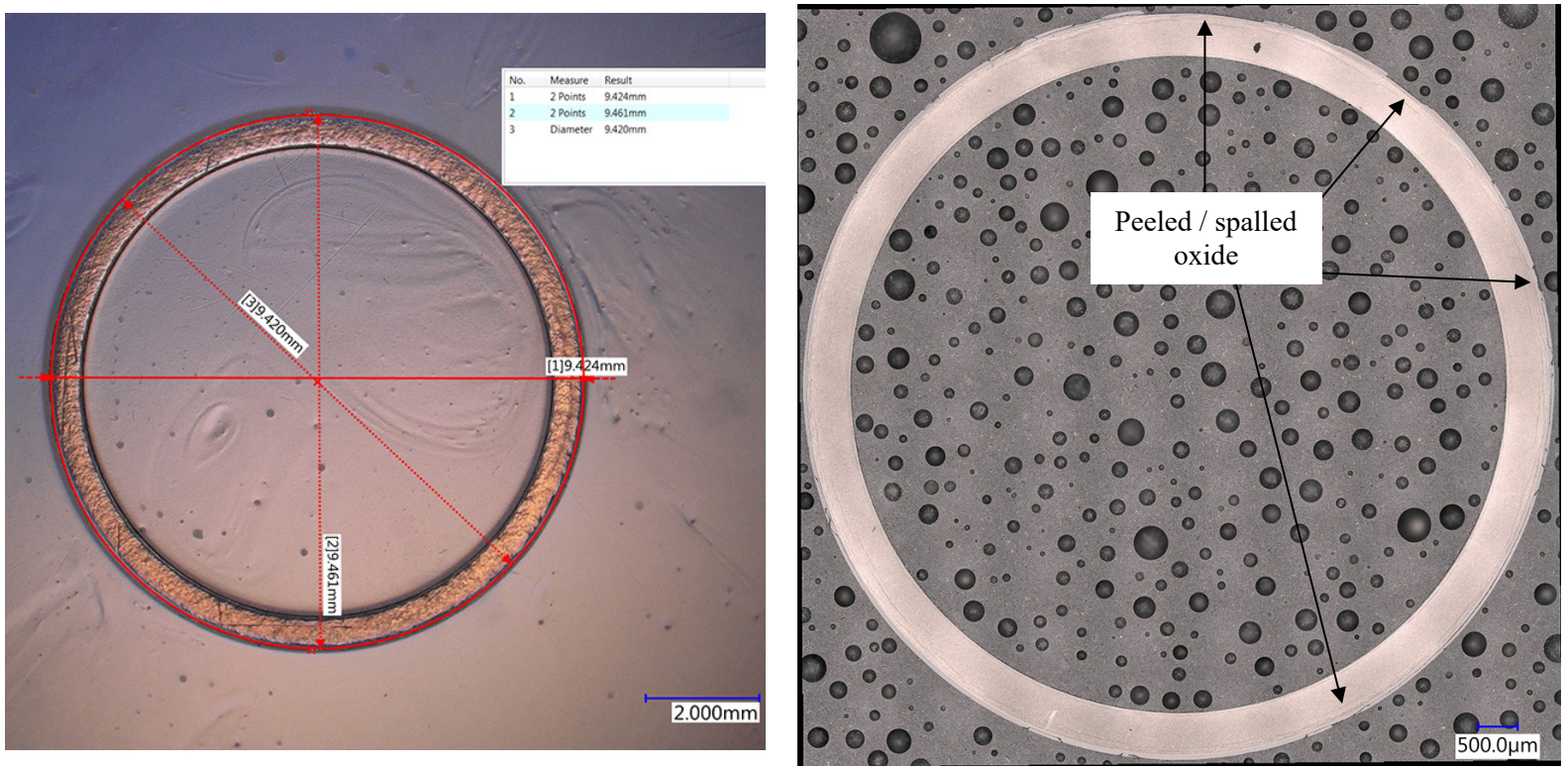

Figure B-10. Defueled overall view, 3D8E14-2655-2674 (left) and 3D8E14-3206-3225 (right) (baseline rod).

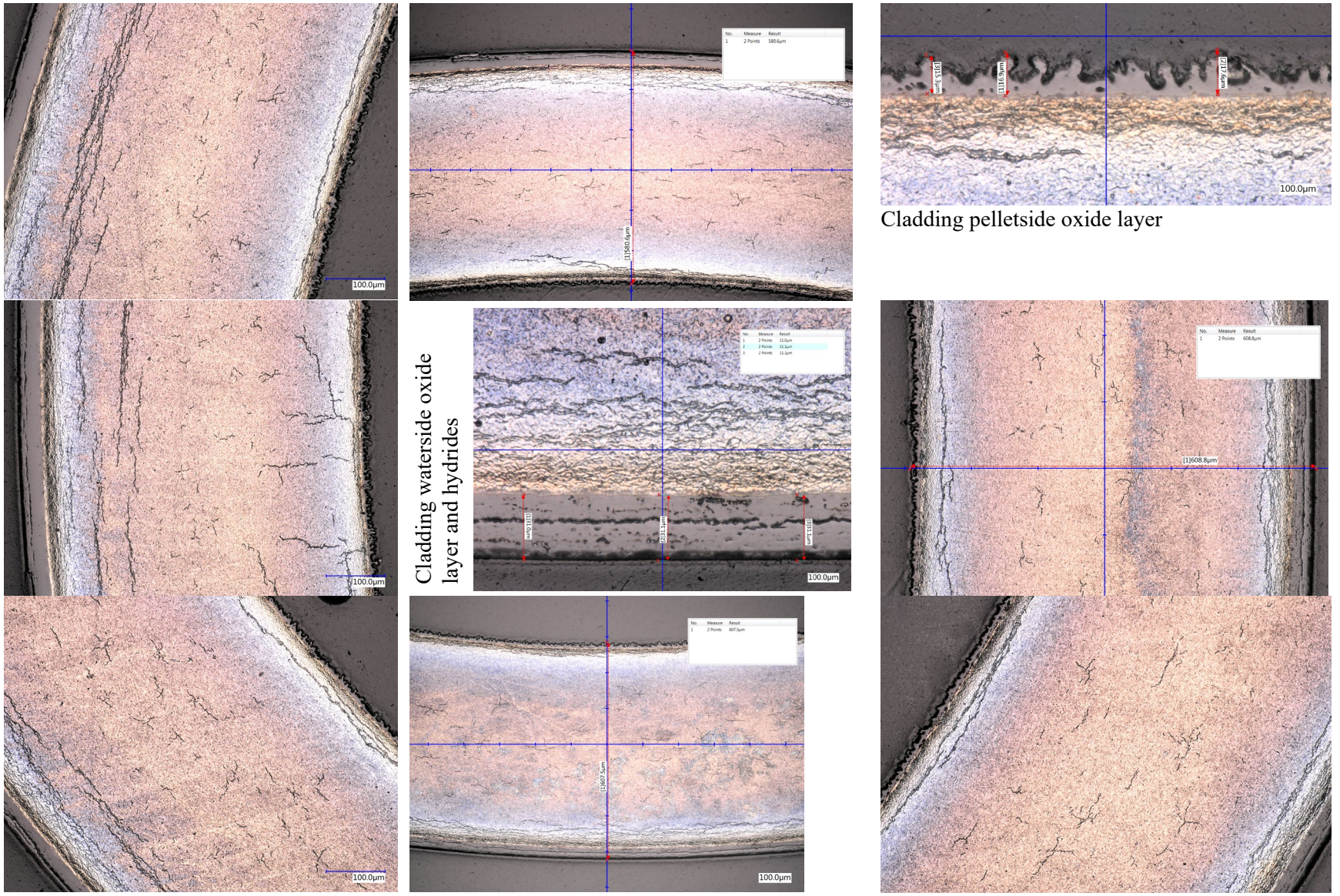

Figure B-11. Magnified areas of 3D8E14-2655-2674 (baseline rod).

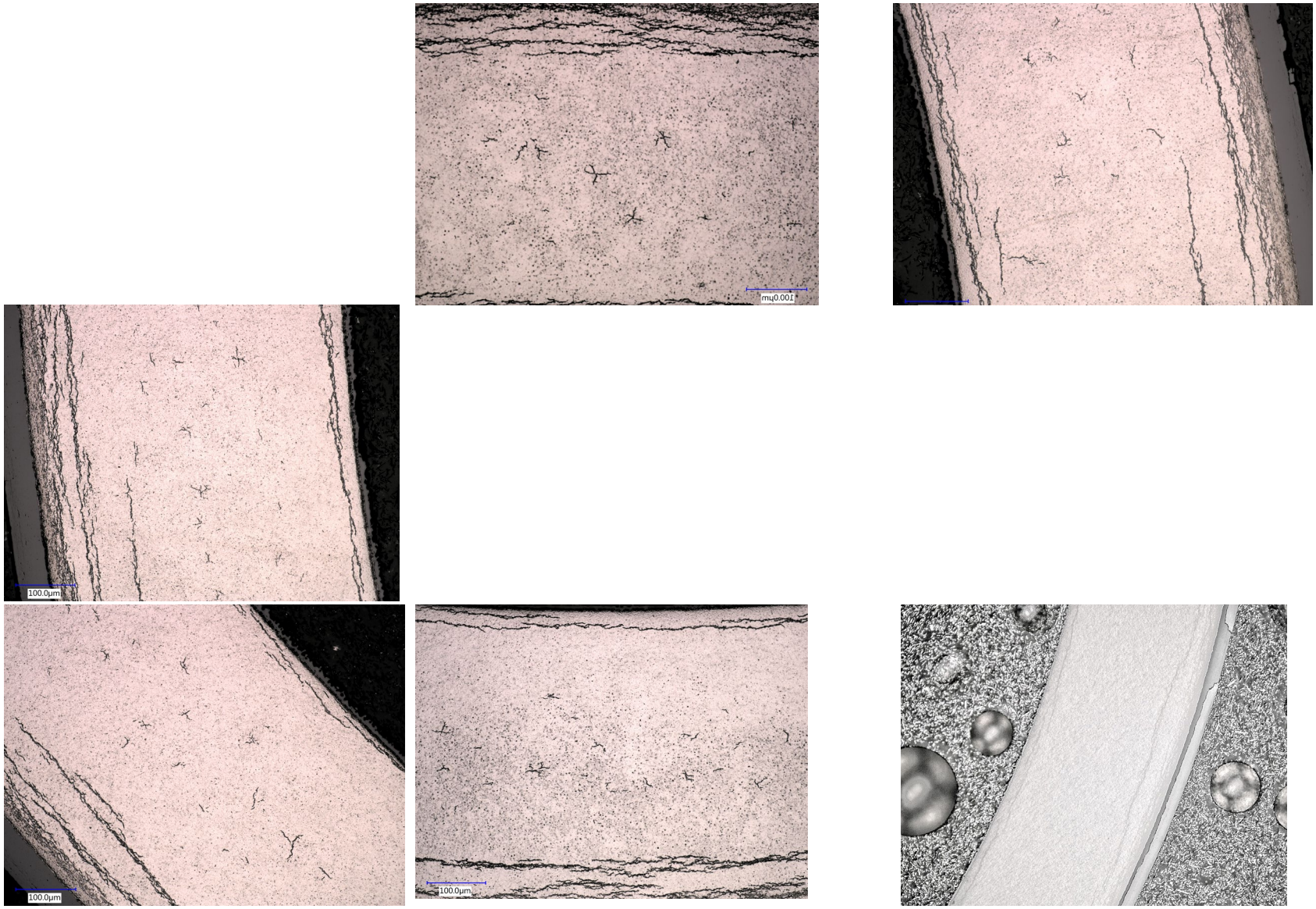

Figure B-12. Magnified areas of 3D8E14-3206-3225 (baseline rod).

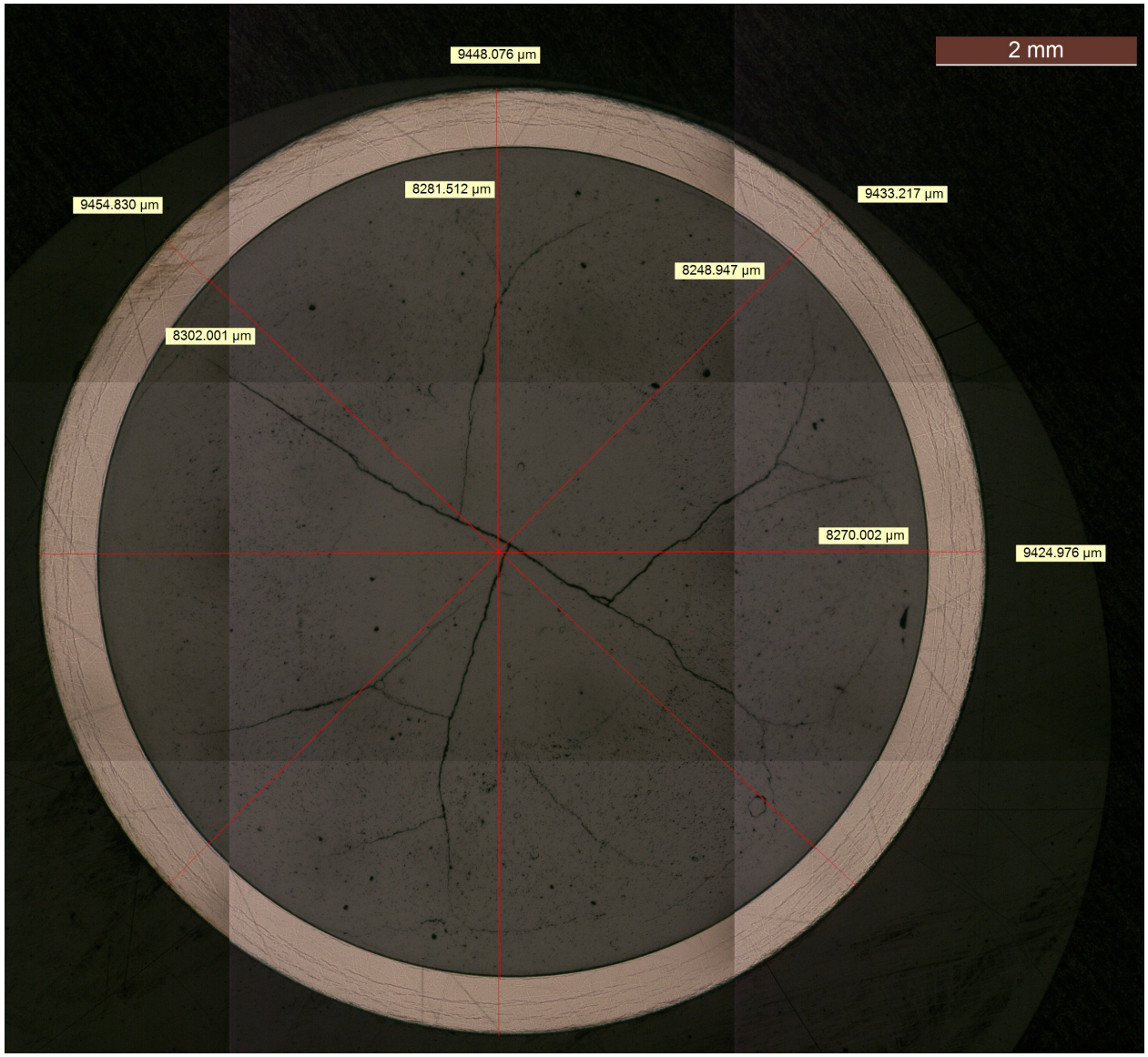

Figure B-13. Fueled overall view, 6U3K09-2616-2635 (baseline rod).

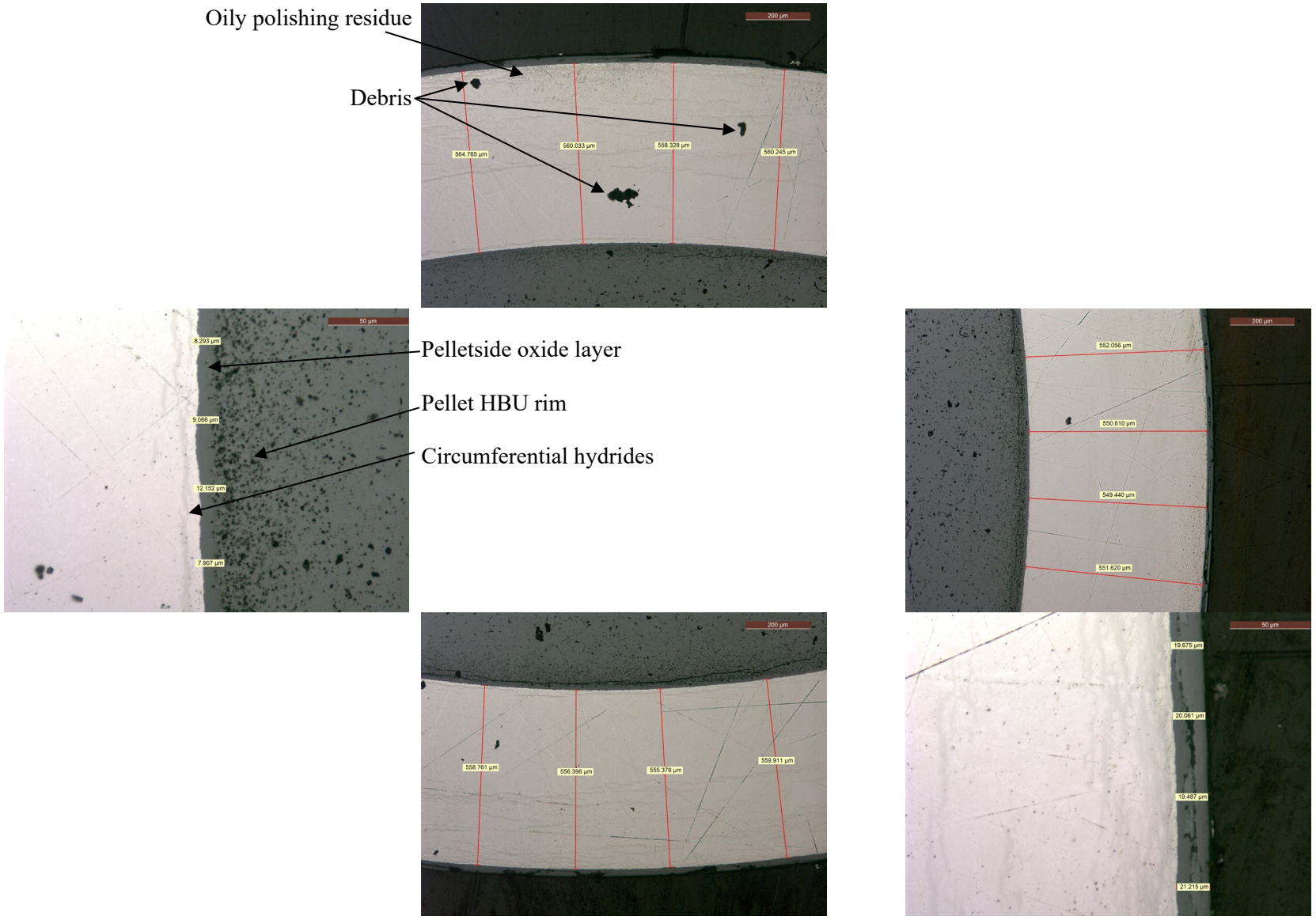

Figure B-14. Magnified views, 6U3K09-2616-2635 (baseline rod).

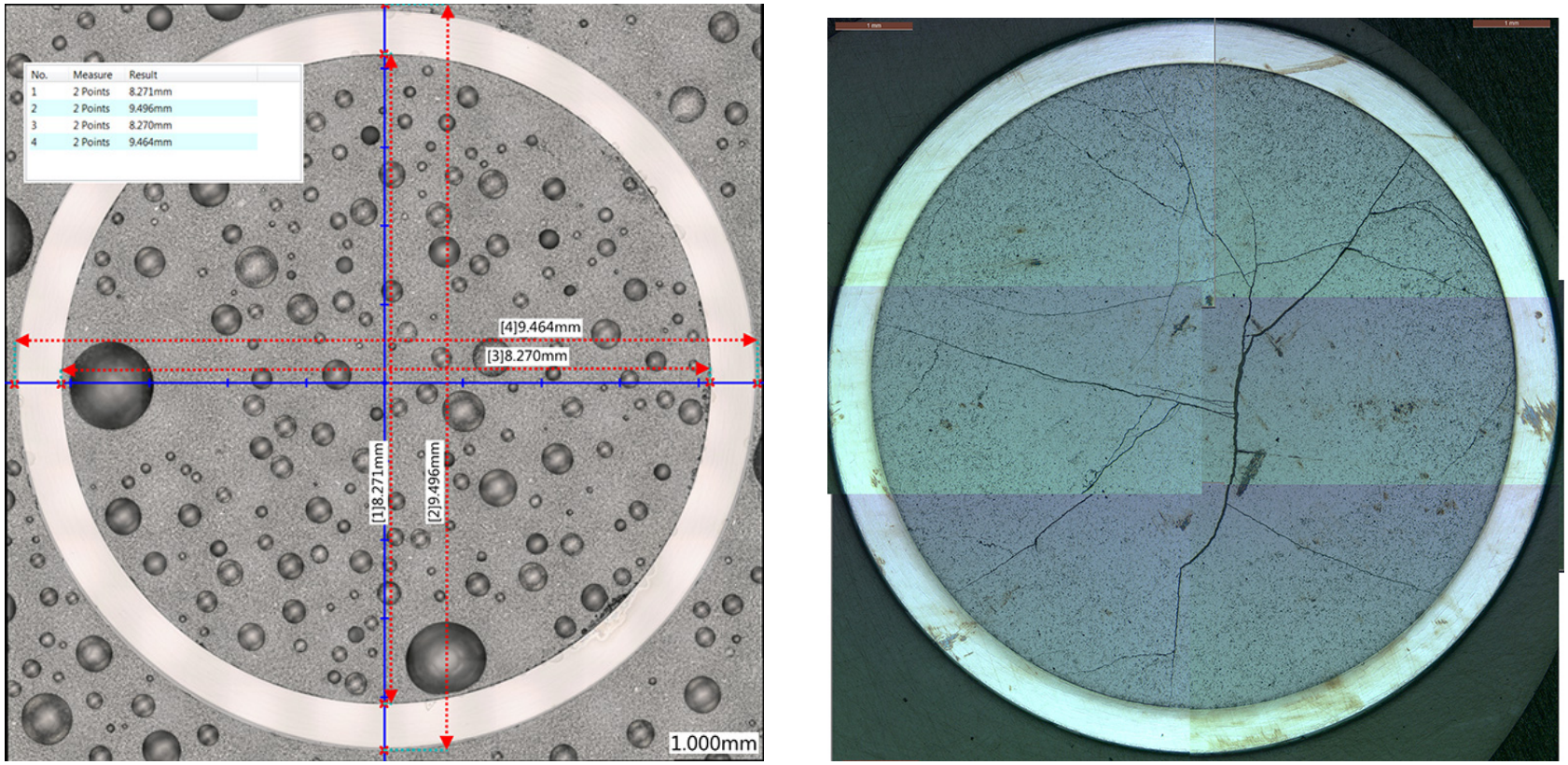

Figure B-15. Defueled (left) and fueled (right) overall views of 3F9N05-3331-3350 (heat-treated).

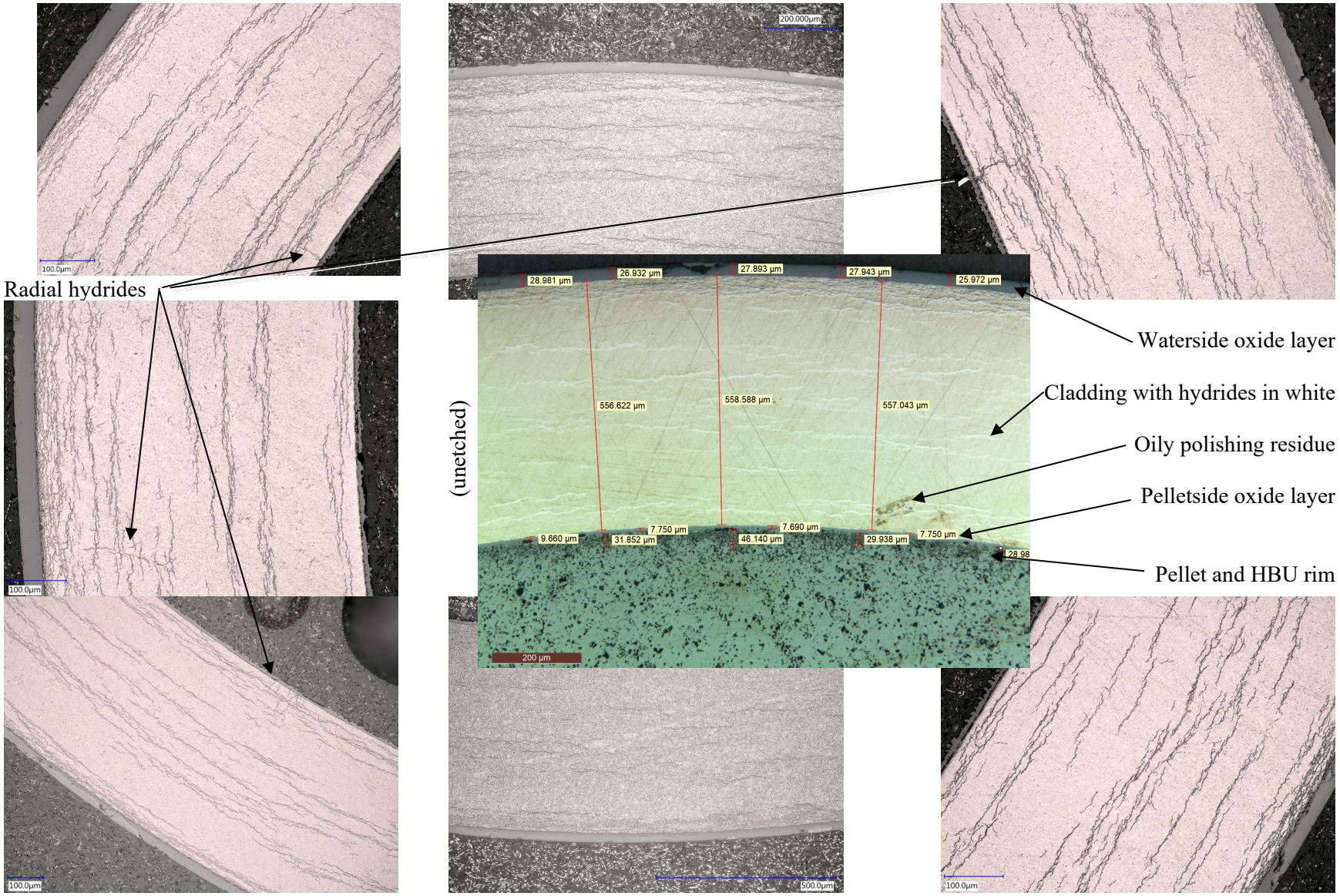

Figure B-16. Magnified views of 3F9N05-2863-2882 (heat-treated).

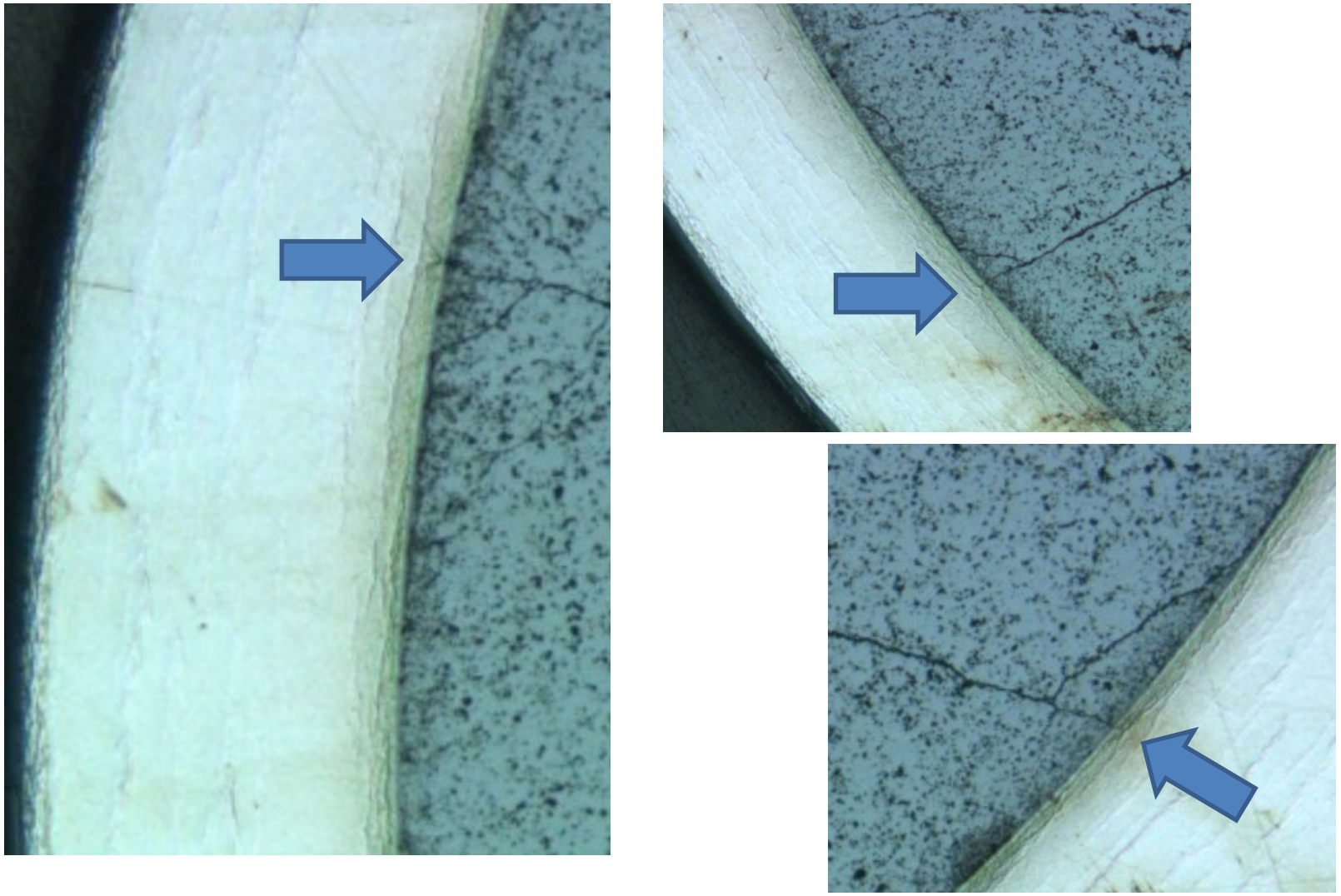

Figure B-17. Magnified views of 3F9N05-2863-2882 (heat-treated) with cladding at pellet crack locations.

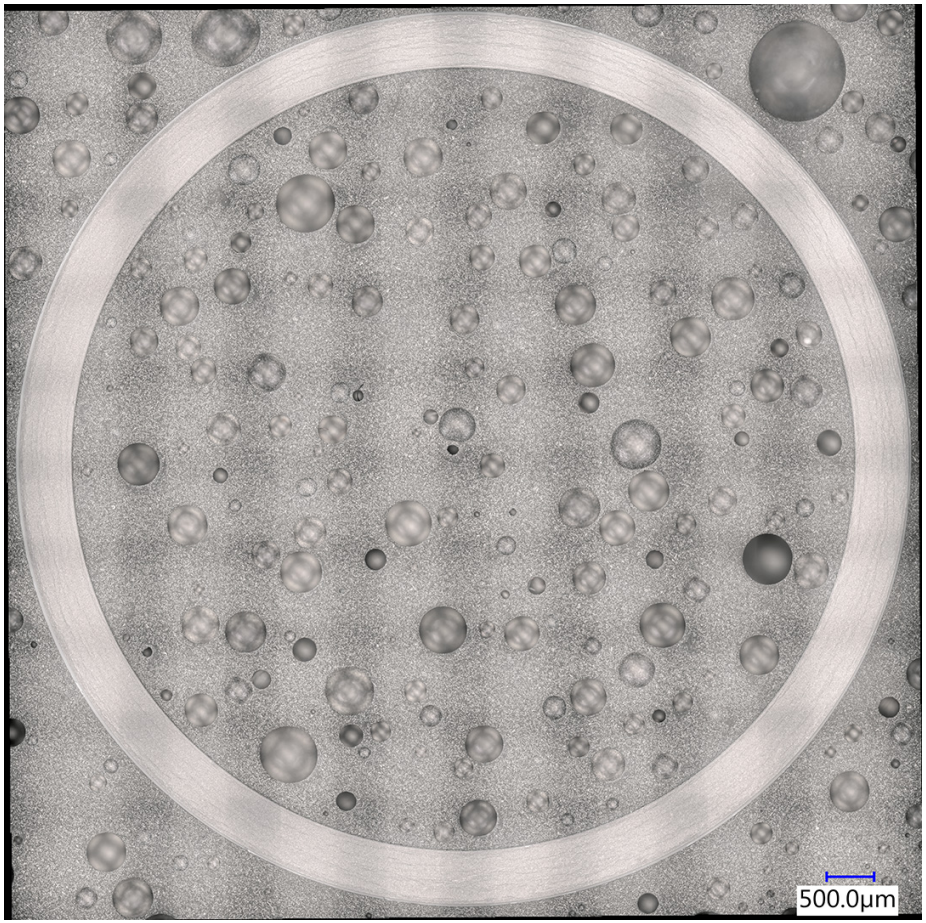

Figure B-18. Defueled overall view of 3F9N05-2863-2882 (heat-treated).

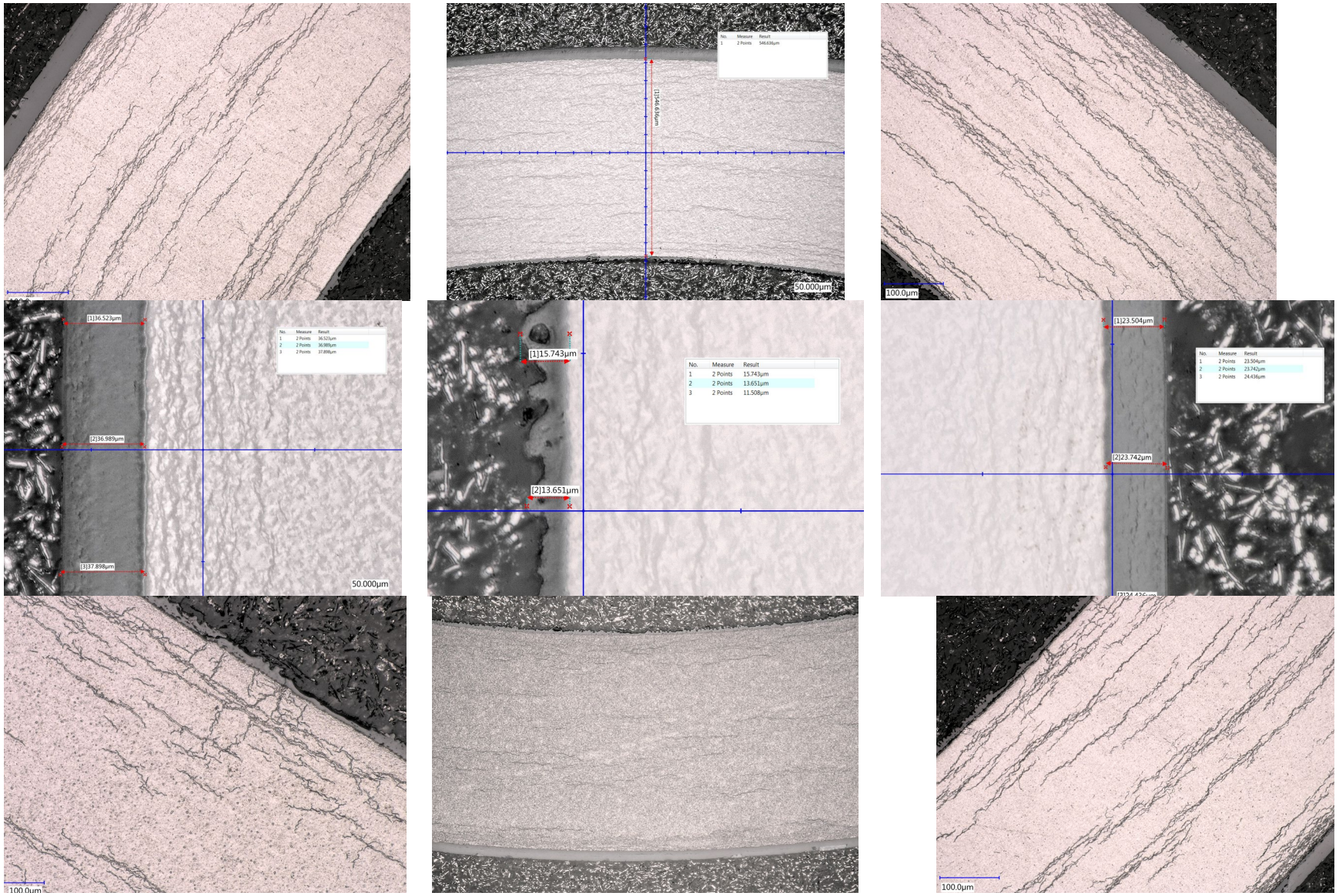

Figure B-19. Magnified views of 3F9N05-2863-2882 (heat-treated).

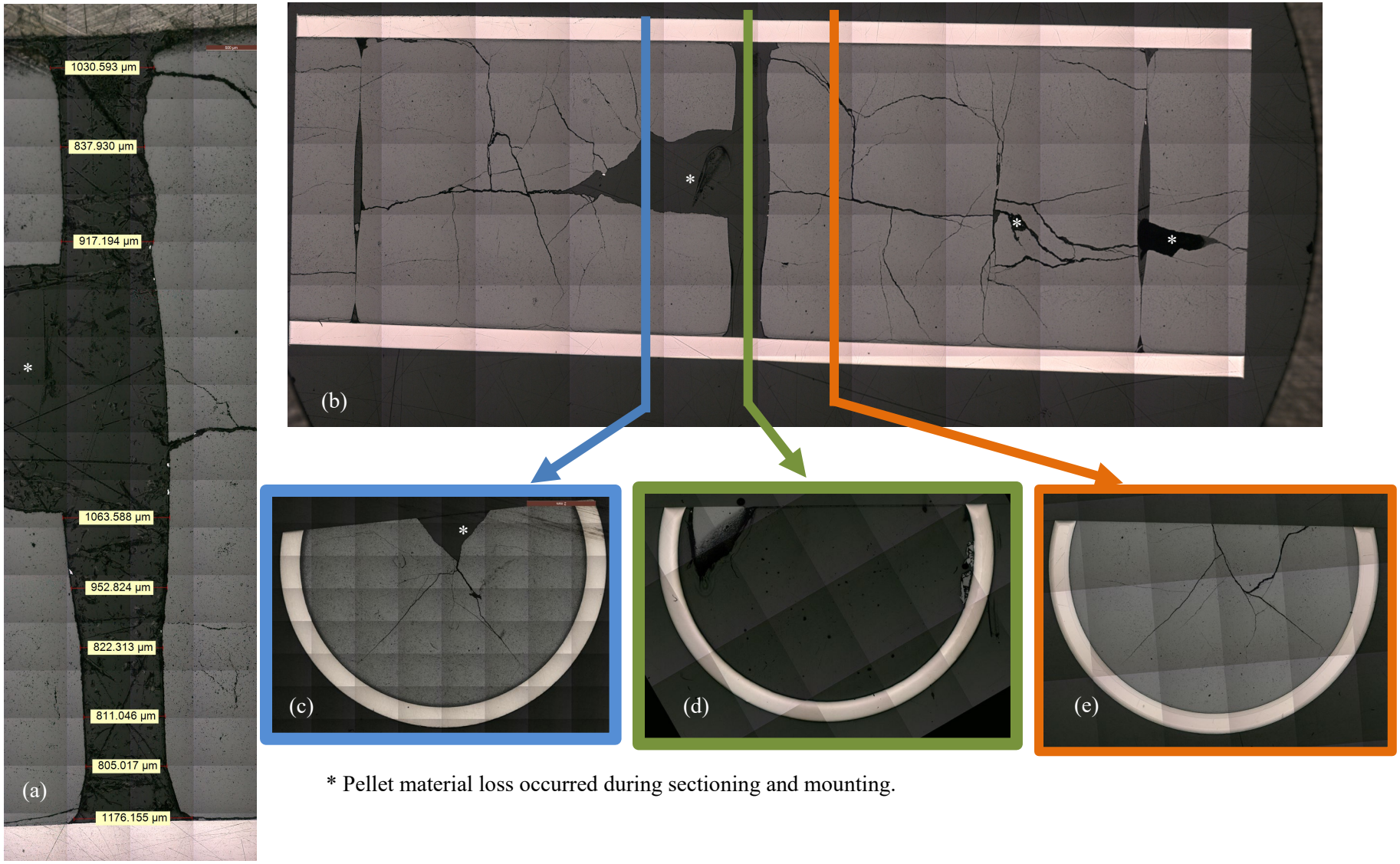

Figure B-20. 3D8E14 at 1,403mm elevation - pellet-pellet (a) gap measurements, (b) axial section view and cross-sectional view locations, (c) cross-sectional view of pellet below the gap, (d) cross-sectional view in the gap, and (e) cross-sectional view of the pellet above the gap.

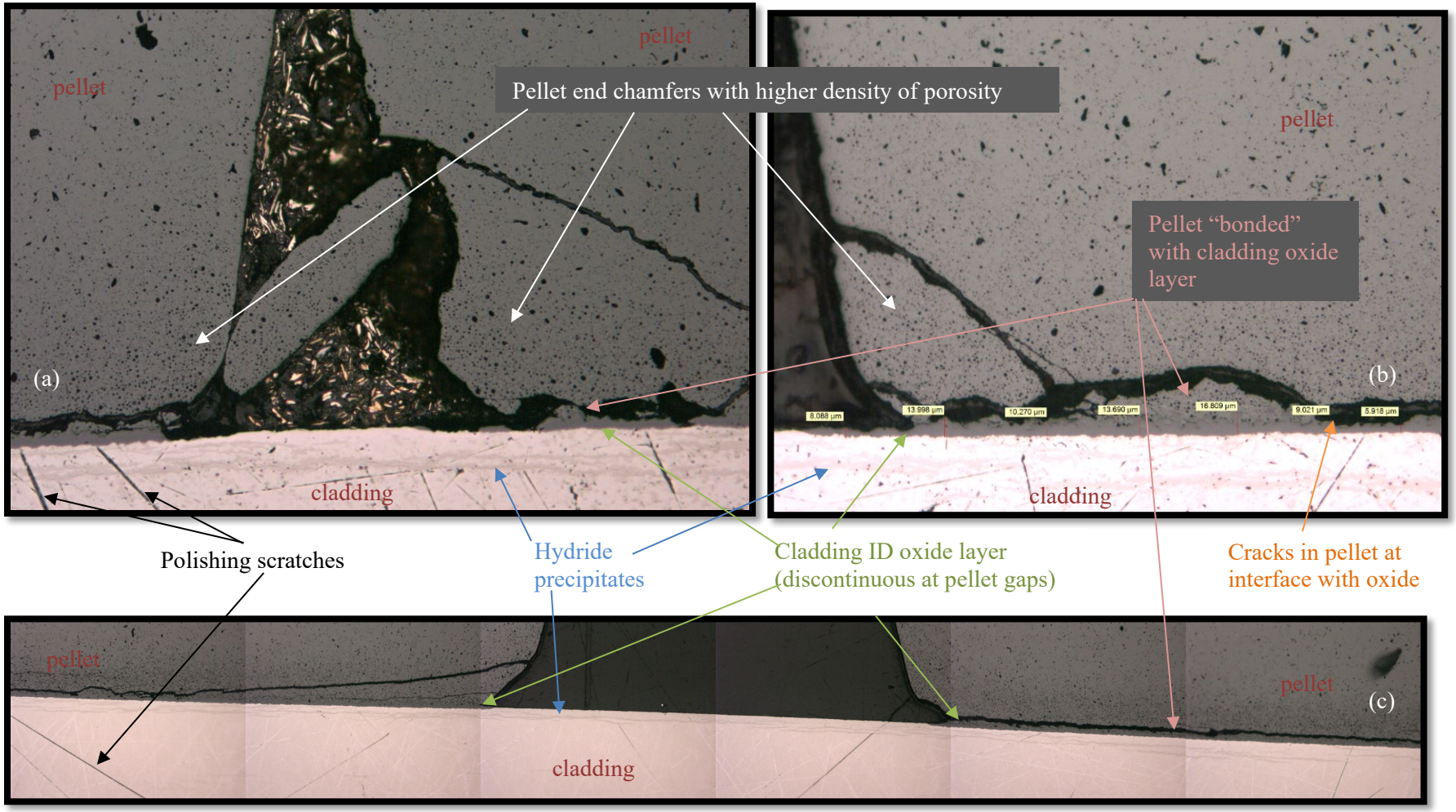

Figure B-20 3D8E14 centered at 1,403mm elevation 200× axial views of three pellet-pellet interface locations showing pellet cracking, HBU rim and corner effects, and cladding ID hydrides.

Table B-6. 3D8E14 centered at 1,403mm elevation measurements.

	Cladding wall thickness (µm)			Waterside oxide layer thickness (µm)			Pelletside oxide layer thickness (µm)			Pellet HBU rim thickness (µm)			Cladding ID (µm)	Cladding OD (µm)	NDE average OD (µm)
	Average	Maximum	Minimum	Average	Maximum	Minimum	Average	Maximum	Minimum	Average	Maximum	Minimum			
Above the gap (~1,408 mm elevation)	568.9	580.2	558.6	14.9	18.3	12.5	11.2	13.7	6.2	85.8	108.0	65.0	8,318.0	9,480.2	9,481.9
In the gap (~1,403 mm elevation)	568.3	576.9	556.9	12.0	12.4	11.6	0	0	0	N/A			8,363.3	9,475.5	9,466.4
Below the gap (~1,398 mm elevation)	569.7	582.9	558.2	12.9	15.6	9.2	11.7	17.5	7.9	85.1	130.5	61.5	8,339.4	9,483.4	9,480.0

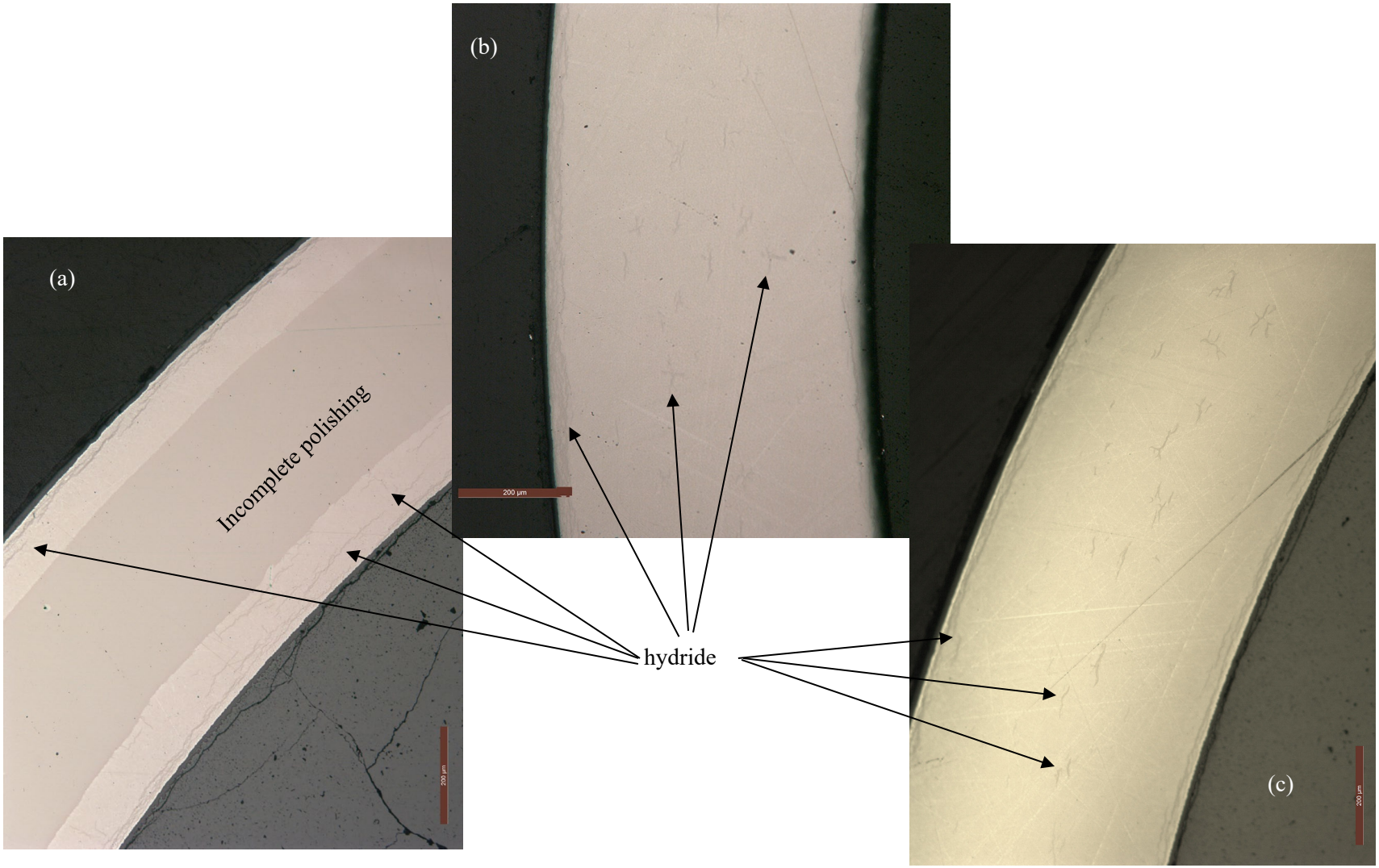

Figure B-21. 3D8E14 centered at 1,403mm elevation, cladding hydride distribution (a) above the gap in the pellet body, (b) in the gap, and (c) below the gap in the pellet body.

B-3.3 Zirc-4-Clad Sister Rods

Figures B-22 through B-24 provide views of F35P17-2735-2754 (heat-treated). Two MET views from one elevation are available for the Phase 1 Zirc-4-clad sister rods. Numerous circumferential hydrides are visible throughout the thickness of the cladding. The visible radial hydrides are short. A large portion of the waterside oxide layer is spalled with an average waterside oxide layer thickness of 81 μm and a maximum thickness of 86 μm at this rod elevation. The spalled layer is almost the full thickness, as shown in Figure B-23, with a ~9 μm layer remaining in the spalled area. The remaining wall thickness in the spalled area is ~510 μm. The pellet cracks are as expected with no messing pellet surface. The pellet HBU rim is 101 μm on average.

F35P17 was manufactured by Westinghouse and used in a lead rod program. It was operated to a rod average burnup of 60 GWd/MTU and the waterside oxide thickness was previously measured at poolside after reactor discharge [B-9]. The waterside oxide thickness was also measured during the sister rod NDE (before the heat-treatment) using two different instruments, the Electric Power Research Institute's F-SECT system and ORNL's eddy current system. At the elevation of F35P17-2735-2754, F-SECT reported ~90 μm and the eddy current reported ~100 μm.

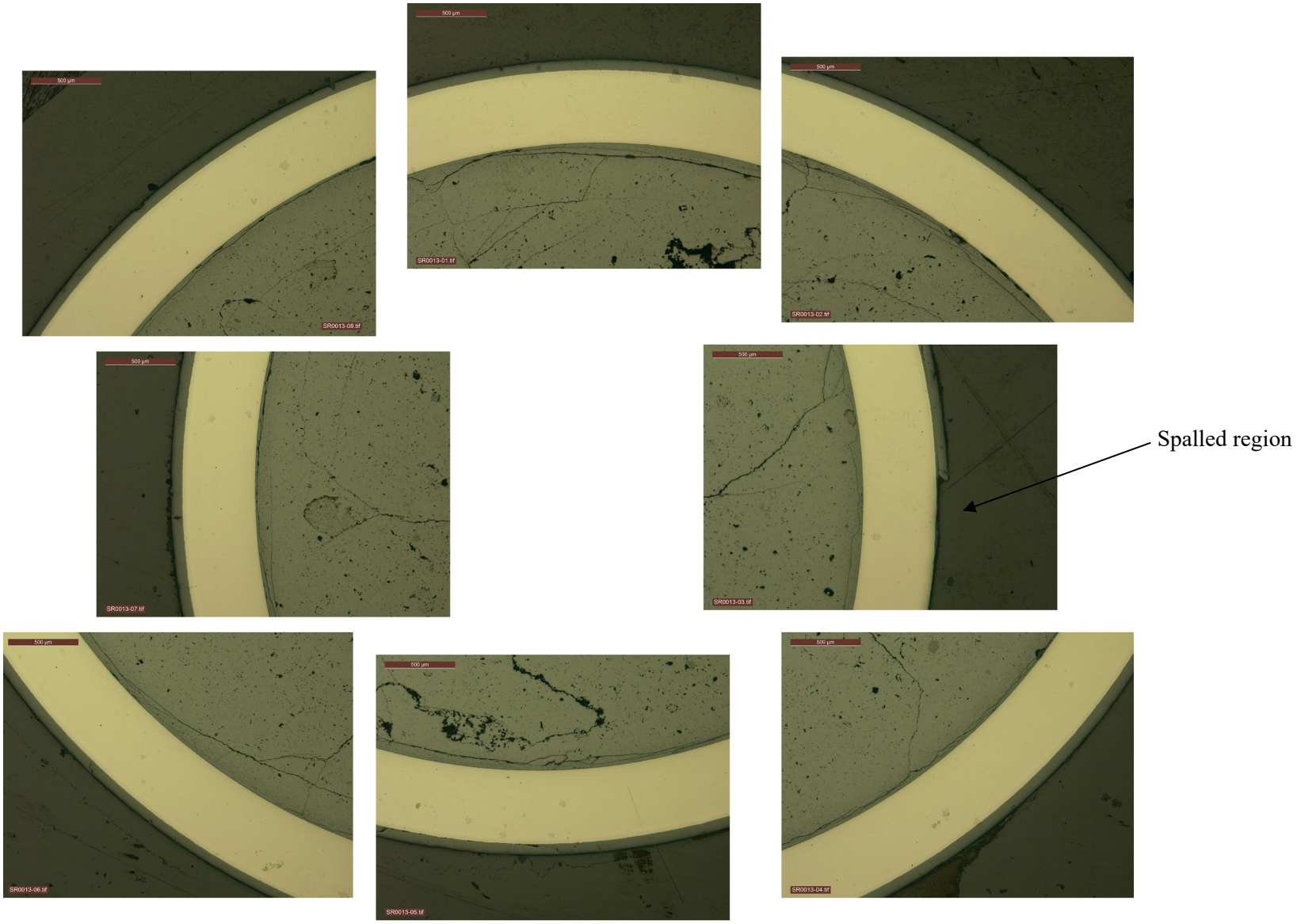

Figure B-22. Mosaic view, fueled, F35P17_2735_2754 (heat-treated).

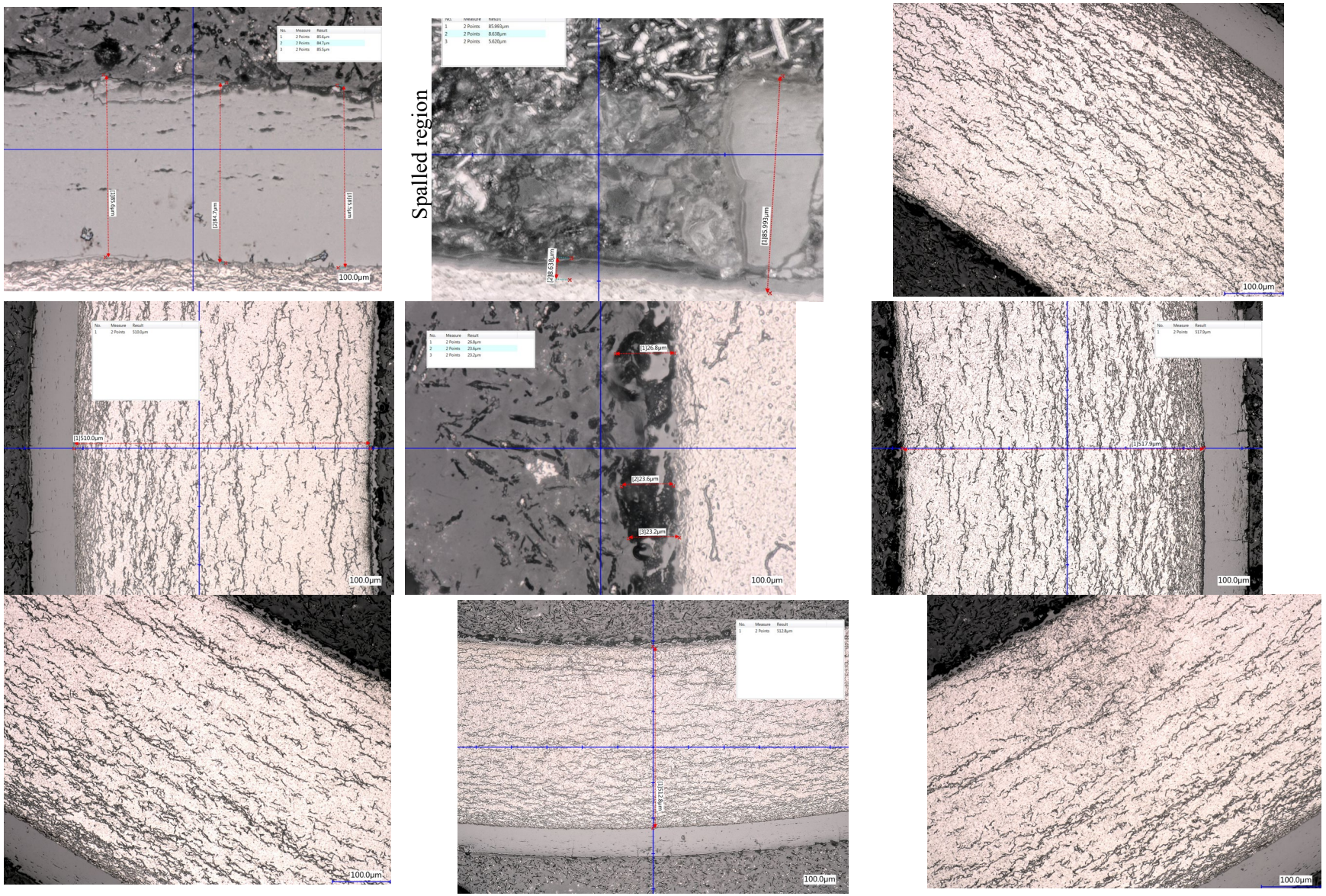

Figure B-23. Magnified views, defueled, F35P17-2735-2754 (heat-treated).

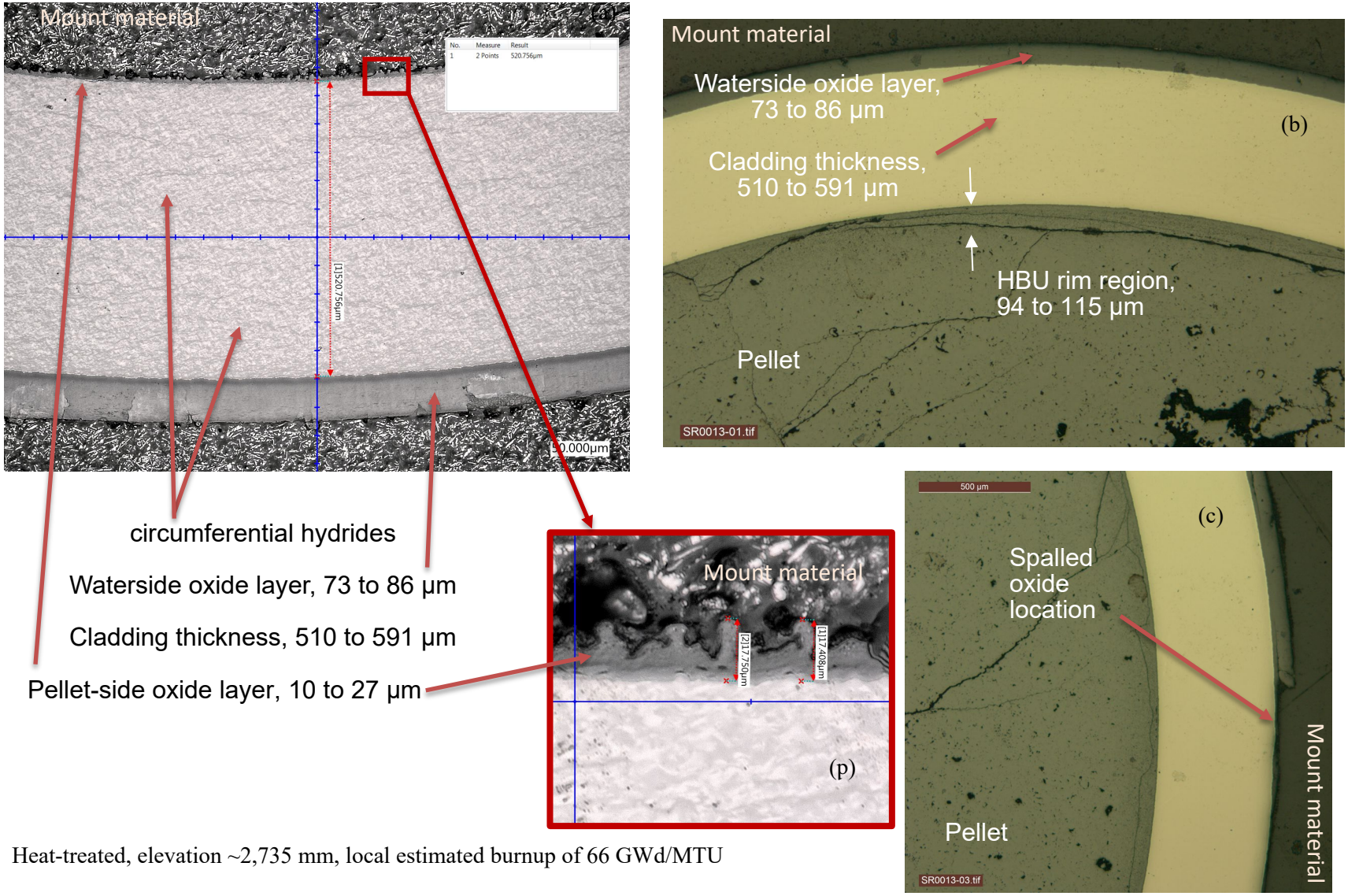

Heat-treated, elevation ~2,735 mm, local estimated burnup of 66 GWd/MTU

Figure B-24. Selected MET views of heat-treated Zirc-4-clad sister rod F35P17

B-3.4 LT Zirc-4-Clad Sister Rods

Figures B-25 through B-27 provide views of 3A1F05-1260-1279, 3A1F05-2735-2754, and 3A1F05-1585-1604. Views from 3A1F05-1260-1279 and 3A1F05-1585-1604 provided measurement data but were not polished well enough to visualize cladding hydrides. 3A1F05 is a baseline rod that was operated to an average rod burnup of 51 GWd/MTU as typical batch supplied fuel. The rod is heavily spalled in the higher burnup elevations, including 3A1F05-2735-2754, as shown in the METs. There is a high density of hydrides near the waterside surface of the cladding and a lower density through the remainder of the wall section. Interior hydrides are circumferentially oriented.

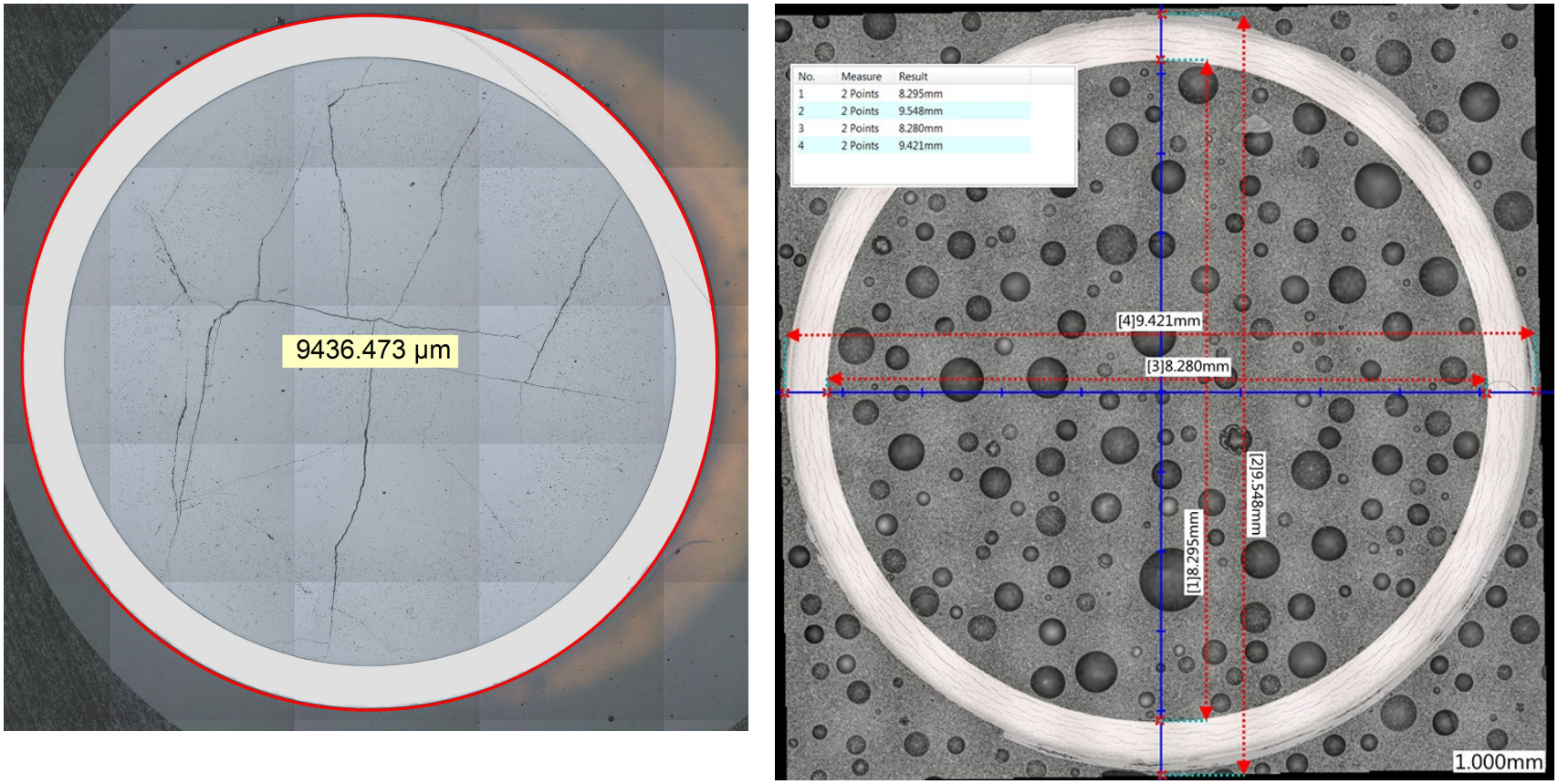

Figure B-25. Fueled overall view of 3A1F05-1260-1279 (left) and 3A1F05-2735-2754 (right) (baseline rod).

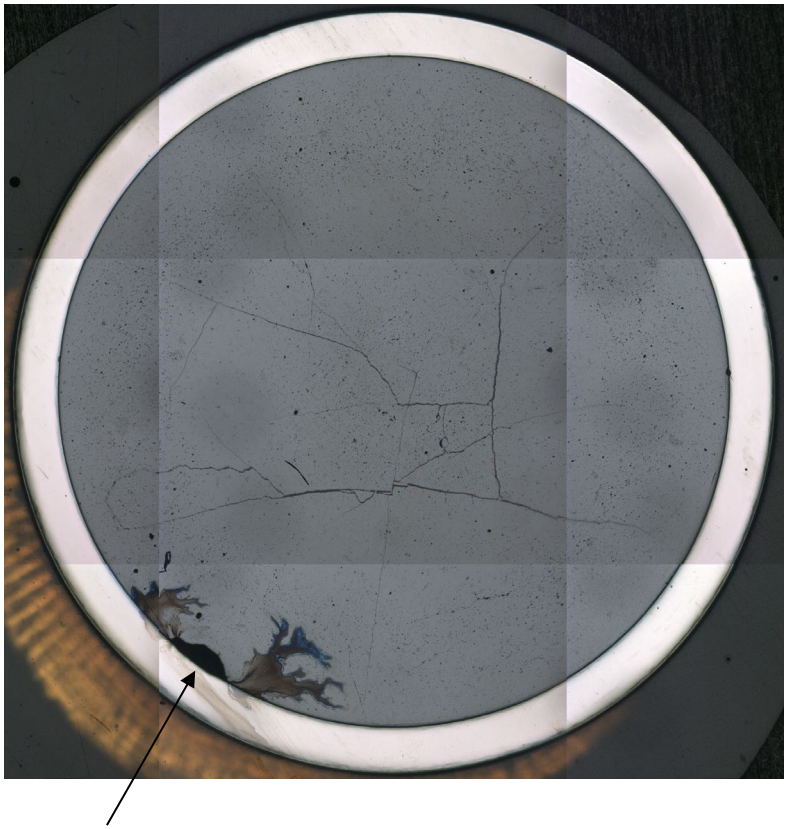

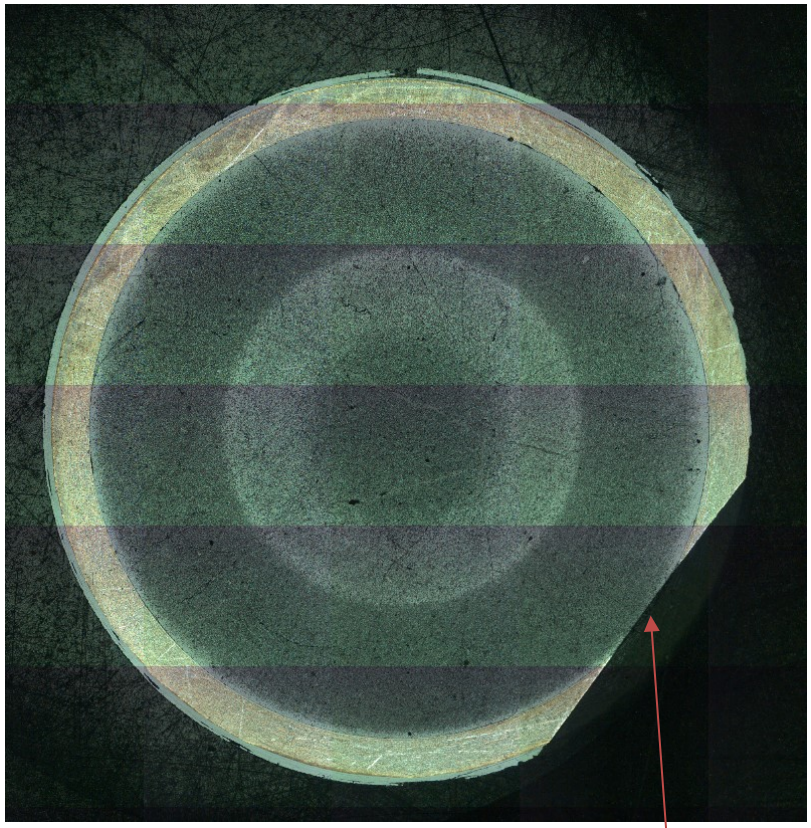

Figure B-26. Fueled overall view of 3A1F05-1585-1604 (left) and 3A1F05-2735-2754 (right) (baseline rod).

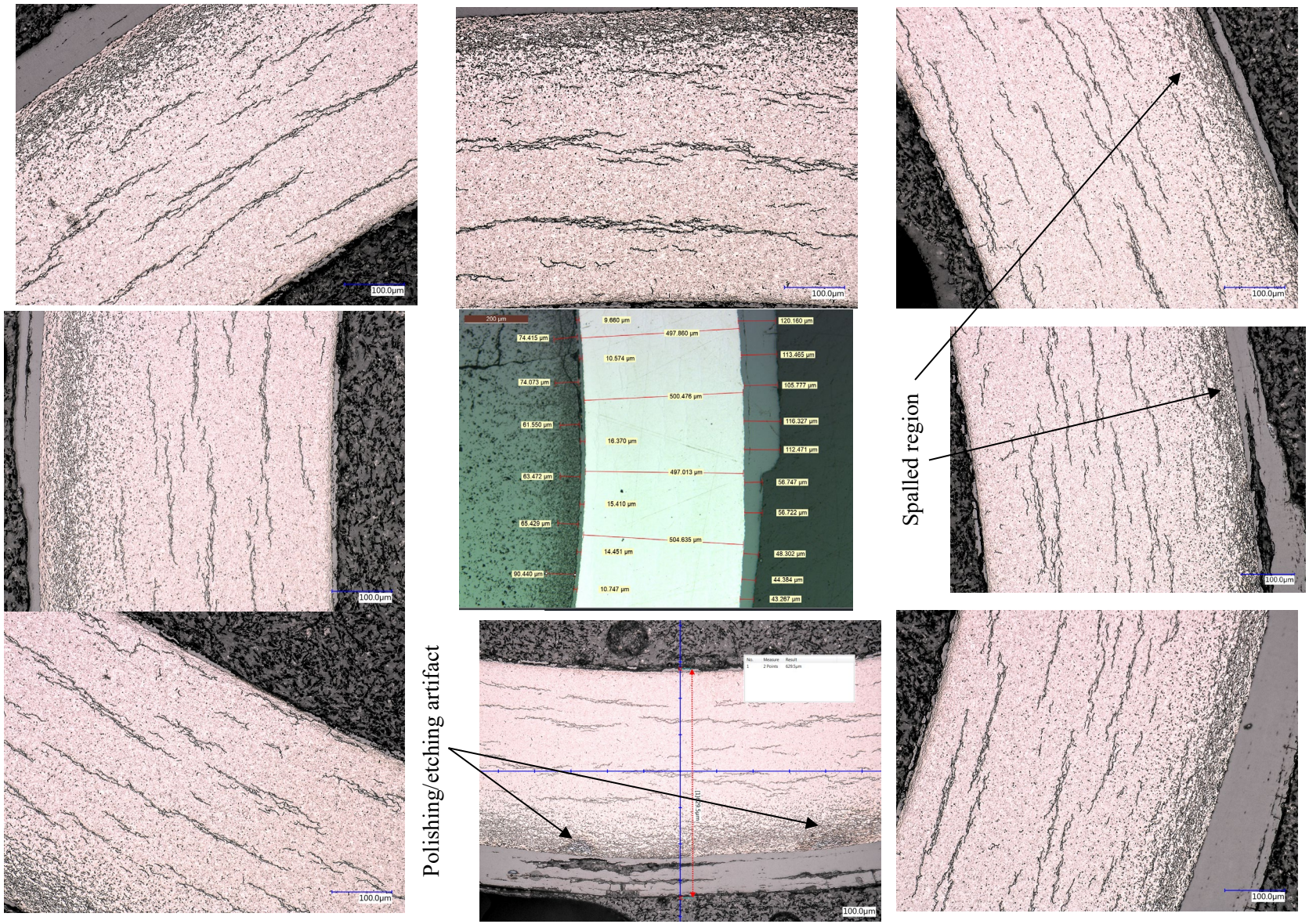

Figure B-27. Magnified views of 3A1F05-2735-2754 (baseline rod).

B-4. CLADDING HYDROGEN MEASUREMENTS (DE.03)

Table B-3 lists the segments that were sub-sectioned to include cladding total hydrogen specimens. The specimens to be used for total hydrogen analysis are 4 mm long. The specimens for total cladding hydrogen analysis will be cut, defueled, and sectioned azimuthally into four quadrants to obtain a minimum sample size of 0.1 g.

As mentioned previously, approximately one-third of the Phase 1 DE-02 segments were sub-sectioned. The total cladding hydrogen specimens are available, and defueling has begun. Calibration of the OHN analyzer is underway and cladding measurements are expected to begin in early FY21.

Part of the testing of the oxygen hydrogen nitrogen (OHN) analyzer is the development of a testing method for the planned conditions. Based on manufacturer's recommendations helium was chosen as the carrier gas. The standard LECO refractory metals procedure was modified slightly to reduce the generation of carbon contamination from each test. In this method a LECO 782-720 high-temperature crucible is filled with approximately 0.050 g of graphite powder. The instrument is fit with a LECO 782-721 lower electrode tip. Samples are placed in a LECO 502-344 nickel basket or a LECO 502-822 nickel capsule for analysis. The system is calibrated with four standards with a certified hydrogen content ranging from 9 to 191 ppm. The ONH collection curves from samples cut from a Zircaloy-2 corrosion coupon are shown in Figure B-28. All indications are that this method is working well and can be applied to irradiated zirconium-based cladding alloy samples early in FY21. Testing is on-going on different zirconium alloy samples to familiarize staff with the operation of the instrument and to establish proper cleaning procedures for samples prior to testing. Modifications to the radiological enclosure are also being finalized. Cold testing of all the necessary maintenance procedures will be performed before to irradiated sample operations.

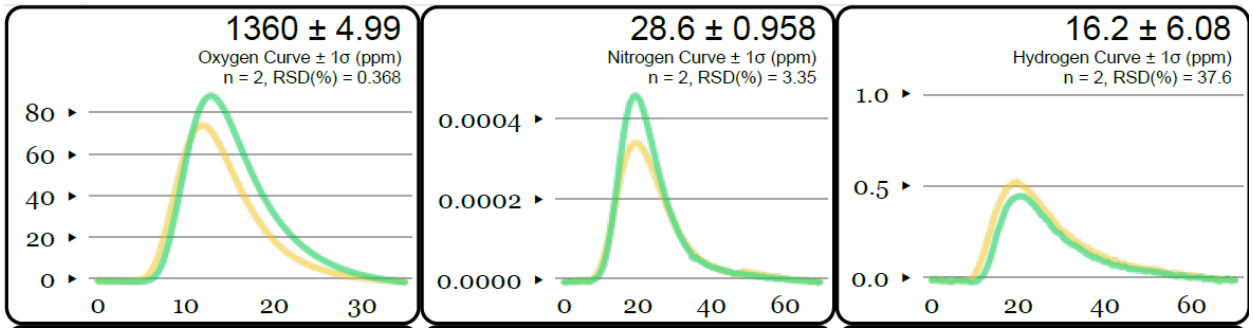

Figure B-28. Oxygen, nitrogen, and hydrogen collection curves from two samples of Zircaloy-2

REFERENCES

[B-1.] High Burnup Dry Storage Cask Research and Development Project: Final Test Plan, contract no. DE-NE-0000593, Electric Power Research Institute, Palo Alto, California (2014).

[B-2.] Saltzstein, Sylvia, et al., Visualization of the High Burnup Spent Fuel Rod Phase 1 Test Plan, SAND2018-8042-O (2018).

[B-3.] Montgomery, R. A. et al., "Post-irradiation Examination Plan for High Burnup Demonstration Project Sister Rods," SFWD-SFWST-2017-000090 ORNL/SR-2016/708, Oak Ridge National Laboratory (2016).

[B-4.] Montgomery, R. A. et al., "Sister Rod Nondestructive Examination Final Report," SFWD-SFWST-2017-000003 Rev. 1 (M2SF-17OR010201021) / ORNL/SPR-2017/484 Rev. 1 (ORNL/SPR-2018/801), Oak Ridge National Laboratory (2019).

[B-5.] Balfour, M. G., et al. *Corrosion of Zircaloy-Clad Fuel Rods in High-Temperature PWRs: Measurement of Waterside Corrosion in North Anna Unit 1, Interim Report, March 1992*, prepared by Westinghouse Electric Corporation for Electric Power Research Institute, TR-1004008, Tier 2 Research Project 2757-1, 1992.